

# State of the Climate in Asia

2021



WEATHER CLIMATE WATER



WORLD  
METEOROLOGICAL  
ORGANIZATION

WMO-No. 1303

Cover photo: Abhushan Gautam / RIMES / 2022.

**WMO-No. 1303**

© World Meteorological Organization, 2022

The right of publication in print, electronic and any other form and in any language is reserved by WMO. Short extracts from WMO publications may be reproduced without authorization, provided that the complete source is clearly indicated. Editorial correspondence and requests to publish, reproduce or translate this publication in part or in whole should be addressed to:

Chair, Publications Board  
World Meteorological Organization (WMO)  
7 bis, avenue de la Paix  
P.O. Box 2300  
CH-1211 Geneva 2, Switzerland

Tel.: +41 (0) 22 730 84 03  
Email: [publications@wmo.int](mailto:publications@wmo.int)

ISBN 978-92-63-11303-0

NOTE

The designations employed in WMO publications and the presentation of material in this publication do not imply the expression of any opinion whatsoever on the part of WMO concerning the legal status of any country, territory, city or area, or of its authorities, or concerning the delimitation of its frontiers or boundaries.

The mention of specific companies or products does not imply that they are endorsed or recommended by WMO in preference to others of a similar nature which are not mentioned or advertised.

The findings, interpretations and conclusions expressed in WMO publications with named authors are those of the authors alone and do not necessarily reflect those of WMO or its Members.

# Contents

- Key messages. . . . . 2**
- Foreword . . . . . 3**
- Preface. . . . . 4**
- Global climate context. . . . . 5**
- Regional climate . . . . . 6**
  - Temperature . . . . . 6
  - Precipitation . . . . . 8
  - Cryosphere . . . . . 9
  - Sea-surface temperature . . . . . 13
  - Ocean heat content . . . . . 14
  - Sea level . . . . . 15
  - Major climate drivers . . . . . 16
- Extreme events. . . . . 19**
  - Tropical cyclones . . . . . 19
  - Heavy precipitation and flooding . . . . . 19
  - Droughts . . . . . 20
  - Heatwaves and wildfires . . . . . 20
  - Other extreme events. . . . . 21
- Climate-related impacts and risks . . . . . 23**
  - Affected population and damage . . . . . 23
  - Agriculture and food security . . . . . 24
  - Impact on the economy. . . . . 24
- Enhancing climate resilience and adaptation policies . . . . . 26**
  - Climate policy and action. . . . . 26
  - Members’ capacities: Climate services and early warning. . . . . 27
- Observational basis for climate monitoring . . . . . 30**
- Data sets . . . . . 31**
- List of contributors. . . . . 33**

# Key messages



The mean temperature over Asia was cooler than the warmest previous year (2020), but it was still between the fifth and seventh warmest year on record, at an estimated 0.86 [0.75–1.02] °C above the 1981–2010 average (1.41 [1.33–1.47] °C above the WMO 1961–1990 reference period for climate change). The mean temperature anomaly over Asia was larger than the global anomaly of 0.42 [0.39–0.47] °C above the 1981–2010 average.



Precipitation was below normal in the western Asia subregion. Reduced rainfall and less snowpack development affected water availability for crops, reducing production.



Most glaciers in the High-Mountain Asia region, particularly in the south-eastern Tibetan Plateau, eastern Himalayas and Pamir Alai, suffered intense mass losses as the result of exceptionally warm and dry conditions in 2021. In the polar regions of Asia, the number of days of snow coverage was at a record low.



The ocean area of WMO Regional Association II (Asia) shows an overall surface ocean warming trend at rates of more than 0.04 °C per year in the area of the Kuroshio Current system, the Arabian Sea, the southern Barents and Kara Seas and the south-eastern Laptev Sea, which is about three times faster than the global surface ocean warming rate.



Cyclone *Shaheen*, that formed in the Indian Ocean and made landfall on 3 October on the northern Oman coast, brought record-breaking rainfall. The intense rainfall resulted in widespread flooding and casualties and large economic losses.



Dust storm events affected different regions in West Asia. Visibility was reduced to less than 1 km at many weather stations and to 20 metres at Bahrain International Airport. Sand and dust storms are also known to induce respiratory illnesses.



There were more than 100 natural hazard events in Asia, of which over 80% were flood and storm events. These resulted in almost 4 000 fatalities, of which around 80% were caused by flooding. Overall, 48.3 million people were directly affected by these hazards, causing total economic damage of US\$ 35.6 billion.



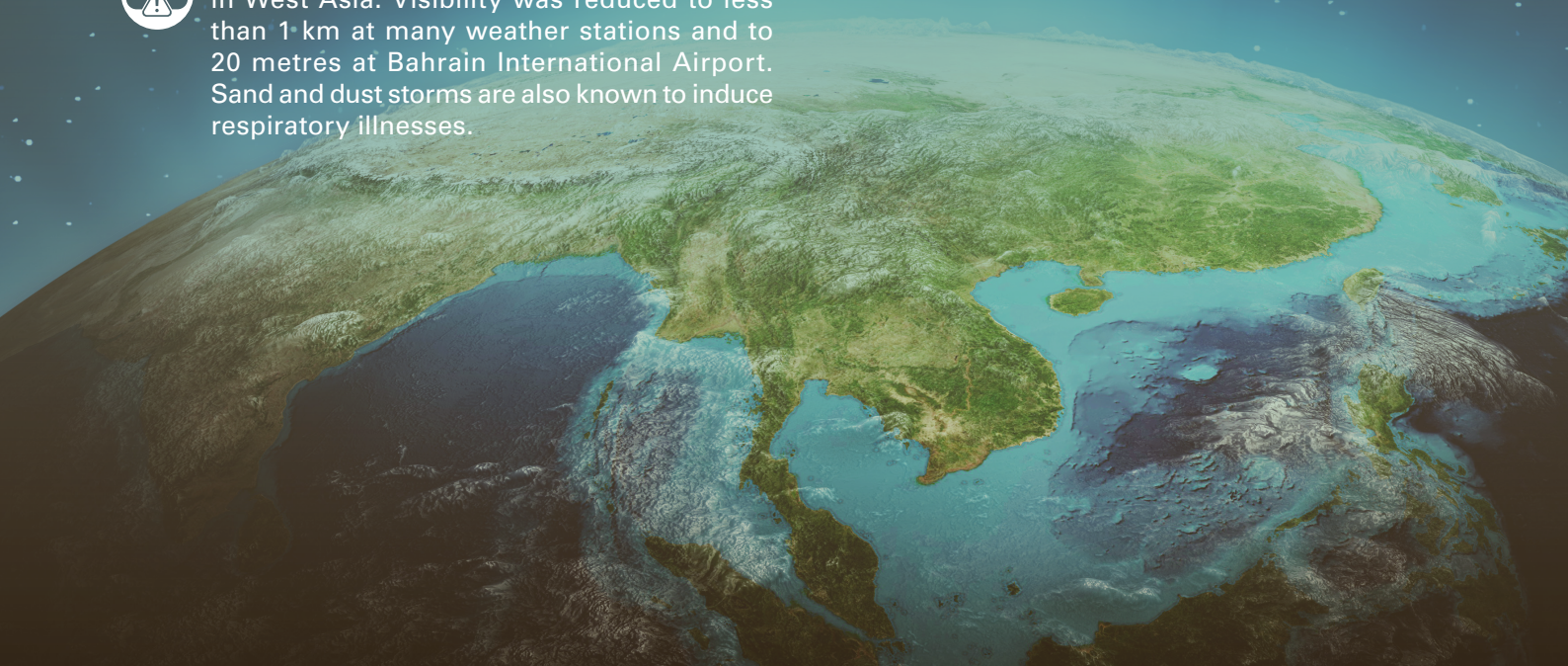
Economic damage from drought has increased by 63%, economic damage from flood has increased by 23%, and from landslides by 147%, compared to the past 20-year average. Strengthening the early warning systems can play a pivotal role in taking anticipatory action, enhancing preparedness and reducing the impact of these hazards.



There is a clear need to prioritize the development of multi-hazard early warning systems and climate forecasts, not only for tackling natural hazards and achieving Sustainable Development Goal (SDG) 13 (Climate Action) (on which insufficient progress has been made towards achieving targets, such as 13.1.1 on the number of deaths, missing persons and directly affected persons attributed to disasters, and 13.1.2 on adoption and implementation of national disaster risk reduction strategies), but also for accelerating progress on several other associated SDGs.



As of June 2022, 31 Parties to the United Nations Framework Convention on Climate Change from the Asia region have submitted a Nationally Determined Contribution (NDC), and mitigation of climate change has been prioritized by all Parties in this region. Their NDCs highlight energy, waste, agriculture and land use/land-use change/forestry (LULUCF) as top priority areas for reducing greenhouse gas emissions.



# Foreword



After the successful publication of the first WMO report on the *State of the Climate in Asia 2020* (WMO-No. 1273) last year, I am pleased to see the timely publication of this second edition. This second report has involved National Meteorological and Hydrological Services (NMHSs) and several research institutions, as well as an increased number of contributing United Nations agencies and international and regional organizations.

The report summarizes the state of the climate, extreme events and their socioeconomic impacts in Asia in 2021. Though temperatures in the region were cooler than the previous year, 2021 was still between the fifth and seventh warmest year on record. Most glaciers in the High-Mountain

Asia region suffered from intense mass losses as the result of exceptionally warm and dry conditions in 2021, and the number of days of snow coverage was at a record low in the polar region of Asia.

Heavy precipitation and tropical cyclones brought casualties and socioeconomic losses affecting a large part of the region, while drought and dust storms had an impact on food security, socioeconomic activities and human health in other parts.

Considering the trends in climate indicators and extreme events shown in this report, and the expected increase of average and heavy precipitation over much of Asia in the future, there is an urgent need to strengthen early warning systems to mitigate the impact associated with increased frequency and intensity of extreme weather and climate events. Despite the continuous efforts to strengthen multi-hazard early warning systems, the present report clearly points out that there are still significant gaps to be addressed to strengthen these systems to reduce the adverse impacts of hydrometeorological hazards in the region.

The information in the present report is built on observing systems coordinated by WMO and its partner organizations. The WMO Integrated Global Observing System (WIGOS) provides basic weather and climate information and the Global Climate Observing System (GCOS) defines a broader set of Essential Climate Variables (ECVs) that are needed to monitor the global climate and support mitigation and adaptation.

While the evidence for climate change in Asia is unequivocal, the most recent Intergovernmental Panel on Climate Change (IPCC) reports show that significant gaps remain in the observation of some variables over the continent, particularly precipitation, but also the basic variables defined in the WMO Global Basic Observing Network (GBON). GBON, and the Systematic Observations Financing Facility that supports it, will provide critically needed observations for numerical weather prediction, and will help to substantially strengthen climate monitoring and early warning systems.

I take this opportunity to congratulate the experts from the region and around the world for leading the scientific coordination and authorship of this report, and thank WMO Members and sister United Nations agencies for their continuous commitment to supporting this publication, through providing input and contributing to the report review process.

Prof. Petteri Taalas  
Secretary-General, WMO

# Preface



Asia is a diverse region with multiple topographies, coastlines and rich natural ecosystems. However, the risk in Asia is expanding. It is also intensifying with climate change impacts, while the ongoing mission of COVID-19 recovery presents further challenges.

In 2021, floods, especially in India, Nepal and China, caused the most serious damage in Asia in terms of fatalities, affected population and economic losses. Unexpected and heavy rains in Nepal also resulted in significant losses to agricultural produce, as the event coincided with a critical period in the harvest season. In Afghanistan, prolonged drought and cascading impacts jeopardized food security. Similarly, rain deficits hit Pakistan while heatwaves engulfed several parts of Asia, including China, Japan and the Russian Federation.

These events shine a spotlight on gaps in adaptation capacity and highlight the urgent need to implement key adaptation solutions. The Glasgow Climate Pact adopted at COP26 in November 2021 boosted adaptation action and added momentum, as it aims for a decade of transformative climate action. However, policy pathways for adaptation must be solidly rooted in scientific evidence.

The Economic and Social Commission for Asia and the Pacific (ESCAP) *Asia-Pacific Disaster Reports 2021* and 2022 estimate that in Asia, the annual investment in adaptation would need to be highest for China, at US\$ 188.8 billion, followed by India at US\$ 46.3 billion, and Japan at US\$ 26.5 billion. As a percentage of the country's GDP, the highest cost is estimated for Nepal, at 1.9%, followed by Cambodia at 1.8%, and India at 1.3%.

Given that floods and tropical cyclones in the region account for the highest economic losses, investment in adaptation must be directed towards prioritizing anticipatory action and preparedness. Notwithstanding the progress in establishing early warning systems, further strengthening is needed as climate change intensifies. Similarly, new infrastructure needs to be made more resilient, alongside improvements in water resources management and dryland agricultural crop production, while nature-based solutions bring durable and wide-ranging benefits. Investing in these solutions would also ensure progress on Sustainable Development Goal (SDG) 13 (Climate Action) and accelerate progress on multiple SDGs, including Goal 1 (No Poverty), Goal 2 (Zero Hunger), Goal 3 (Good Health and Well-being), Goal 9 (Industry, Innovation and Infrastructure) and Goal 11 (Sustainable Cities and Communities).

In this context, the *State of the Climate in Asia 2021* is timely, as it unpacks the interconnections between climate indicators and the SDGs, and helps bridge gaps between science and policy practice. ESCAP and WMO, working in partnership, will continue to invest in raising climate ambition and accelerating the implementation of climate policy actions. To this end, the ESCAP Risk and Resilience Portal, which uses the latest climate information and identifies risk hotspots and adaptation measures by country and subregions provides much of the evidence base for this report. Policymakers are invited to use the Portal to help streamline evidence-based decision-making.

Armida Salsiah Alisjahbana  
Under-Secretary-General of the United Nations and Executive Secretary of ESCAP

# Global climate context

The global annual mean temperature in 2021 was  $1.11 \pm 0.13$  °C above the 1850–1900 pre-industrial average – less warm than in some recent years, owing to cooling La Niña conditions at the start and end of the year. The year 2021 was between the fifth and seventh warmest year on record according to six data sets (Figure 1). The past seven years, 2015 to 2021, were the seven warmest years on record. The year 2016, which started during a strong El Niño, remains the warmest year on record in most data sets.

Atmospheric concentrations of the three major greenhouse gases reached new record highs in 2020, with levels of carbon dioxide (CO<sub>2</sub>) at  $413.2 \pm 0.2$  parts per million (ppm), methane (CH<sub>4</sub>) at  $1\,889 \pm 2$  parts per billion (ppb) and nitrous oxide (N<sub>2</sub>O) at  $333.2 \pm 0.1$  ppb – respectively 149%, 262% and 123% of pre-industrial (before 1750) levels. Real-time data from specific locations, including Mauna Loa (Hawaii) and Cape Grim (Tasmania) indicate that levels of CO<sub>2</sub>, CH<sub>4</sub> and N<sub>2</sub>O continued to increase in 2021. Increasing greenhouse gas concentrations lead to an accumulation of heat in the climate system, much of which is stored in the ocean.

Over the past two decades, the ocean warming rate strongly increased and the ocean heat content in 2021 was the highest on record. Ocean warming and accelerated loss of ice mass from the ice sheets contributed to the rise of the global mean sea level by 3.3 mm per year between 1993 and 2021, and 4.5 mm per year between 2013 and 2021, reaching a new record high in 2021. The ocean absorbs about 23% of annual anthropogenic emissions of CO<sub>2</sub> into the atmosphere, thereby helping to alleviate overall warming; however, CO<sub>2</sub> reacts with seawater and lowers its pH. This process, known as ocean acidification, affects many organisms and ecosystem services, and threatens food security by endangering fisheries and aquaculture.<sup>1,2</sup>

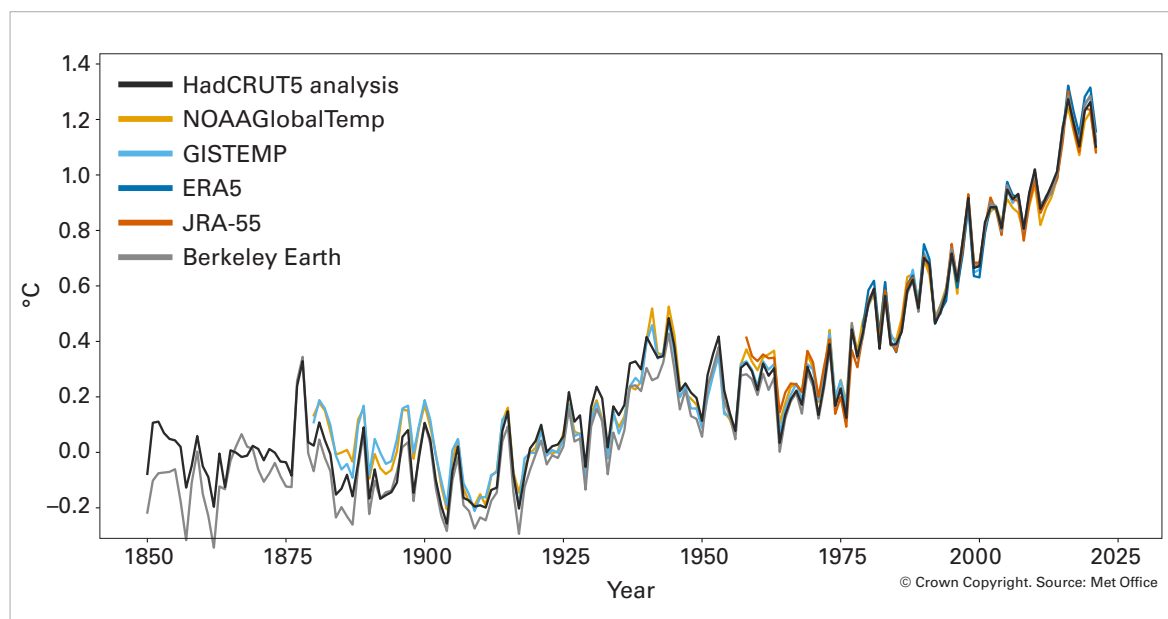


**Figure 1.** Global annual mean temperature difference from pre-industrial conditions (1850–1900) for six global temperature data sets.

For further explanation and details of the data sets, see [State of the Global Climate 2021](#) (WMO-No. 1290).

Source: Met Office, United Kingdom of Great Britain and Northern Ireland

# Regional climate

The following sections provide analysis of key indicators of the state of the climate in Asia during 2021. One important such indicator, temperature, is described in terms of anomalies, or departures from a reference period. For global mean temperature, the Sixth Assessment Report (AR6) of the Intergovernmental Panel on Climate Change (IPCC)<sup>3</sup> uses the reference period 1850–1900 for calculating anomalies in relation to pre-industrial levels. However, the pre-industrial reference period cannot be used as a baseline for calculating regional anomalies, due to insufficient data for calculating region-specific averages prior to 1900. Regional temperature anomalies are therefore expressed relative to the 30-year 1961–1990 reference period. This is the fixed reference period recommended by WMO as a consistent and stable reference period for assessing long-term climate change, especially for temperature. The 1981–2010 climatological standard normal period is also used in some cases, for computing anomalies in temperature and other indicators with reference to more recent climate average conditions. In the present report, exceptions to the use of these baseline periods for the calculation of anomalies, where they occur, are explicitly noted.

## TEMPERATURE

The temperature at Earth’s surface, in conjunction with precipitation, has a great impact on natural systems and on humans. In 2021, the mean temperature over Asia<sup>4</sup> was cooler than in 2020, although it was still between the fifth and seventh warmest year on record (Figure 2). The temperature is estimated to have been 0.86 [0.75–1.02] °C above the 1981–2010 average and 1.41 [1.33–1.47] °C above the 1961–1990 average (WMO reference period for assessing climate change), depending on the data set considered. The mean temperature anomaly over Asia was larger than the global anomaly of 0.42 [0.39–0.47] °C above the 1981–2010 average. Mean temperatures were above the 1981–2010 normal around West and East Asia, and below normal in central Siberia, the far eastern part of the Russian Federation and some parts of South Asia (Figure 3). Reflecting this distribution, the annual mean temperature in China<sup>5</sup> and Bahrain in 2021 was the highest on record (since the beginning of the twentieth century) and was also the highest in the United Arab Emirates since 2003 and the second highest in Saudi Arabia since 1985. Moreover, 2021 was the warmest year in Hong Kong, China, since records began in 1884.

Over the long term, a warming trend has emerged in Asia in the latter half of the twentieth century (Figures 2 and 4). In the two recent sub-periods (1961–1990 and 1991–2020), the warming trends in Asia, which is the continent with the largest land mass extending to the polar region, have exceeded the global mean value – reflecting that temperature increase over land is larger than over the ocean, as stated in the IPCC AR6 report. The warming trend in Asia in 1991–2020 was larger than the warming trends in the 1961–1990 period and previous 30-year periods (Figure 4).

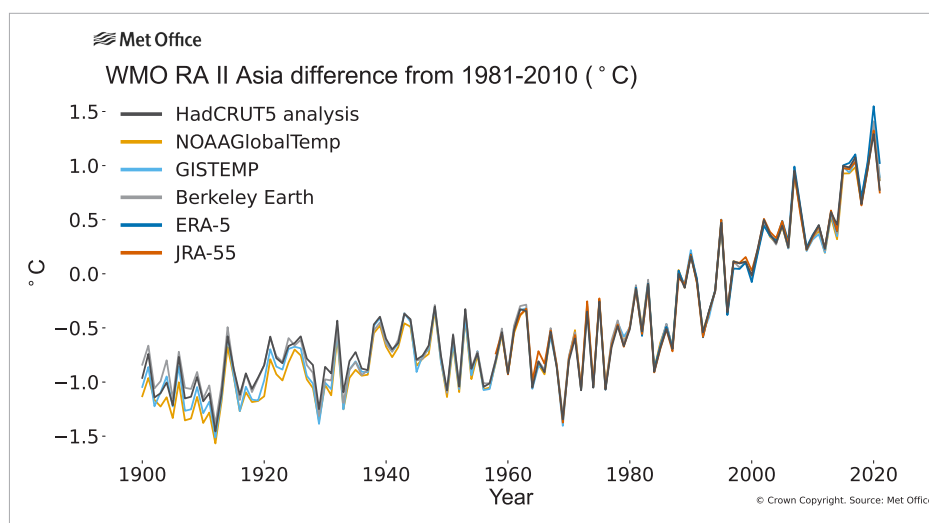


**Figure 2.** Annual mean temperature anomalies (°C), 1900–2021, averaged over Asia, relative to the 1981–2010 average, for six global temperature data sets as indicated in the legend.

Source: MetOffice, United Kingdom  
Note: HadCRUT5, Berkeley Earth, NOAAGlobalTemp and GISTEMP are based on in situ observations. ERA-5 and JRA-55 are reanalysis data sets. For details of the data sets and plotting, see [Temperature](#) data at the end of the present report.

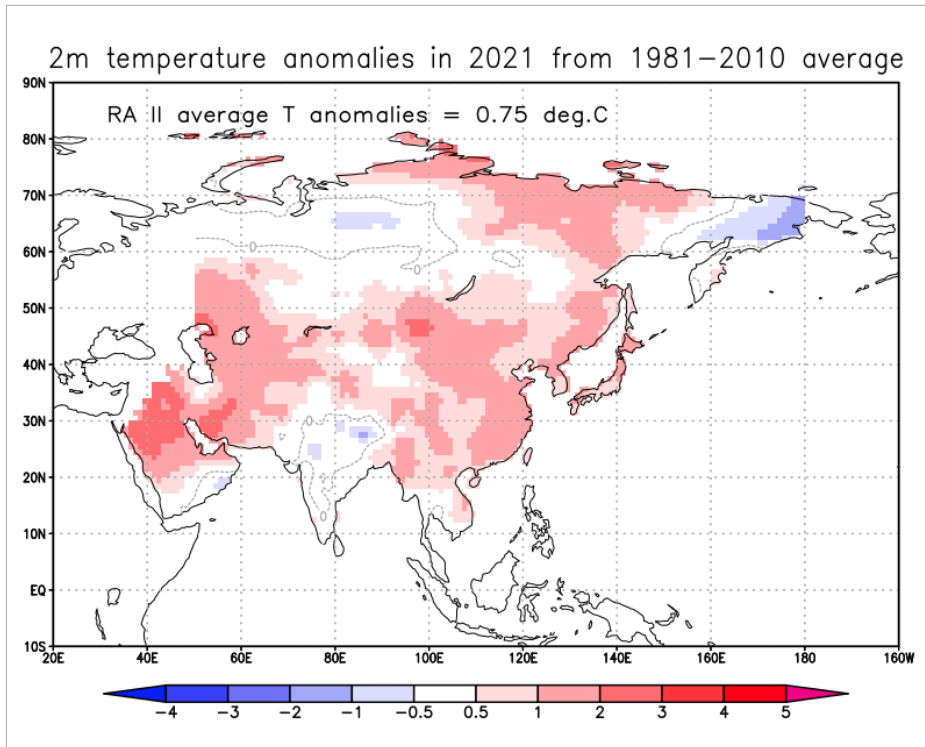


**Figure 3.** Temperature anomalies (°C) relative to the 1981–2010 long-term average from the JRA-55 reanalysis for 2021.  
*Source:* Tokyo Climate Center, Japan Meteorological Agency.

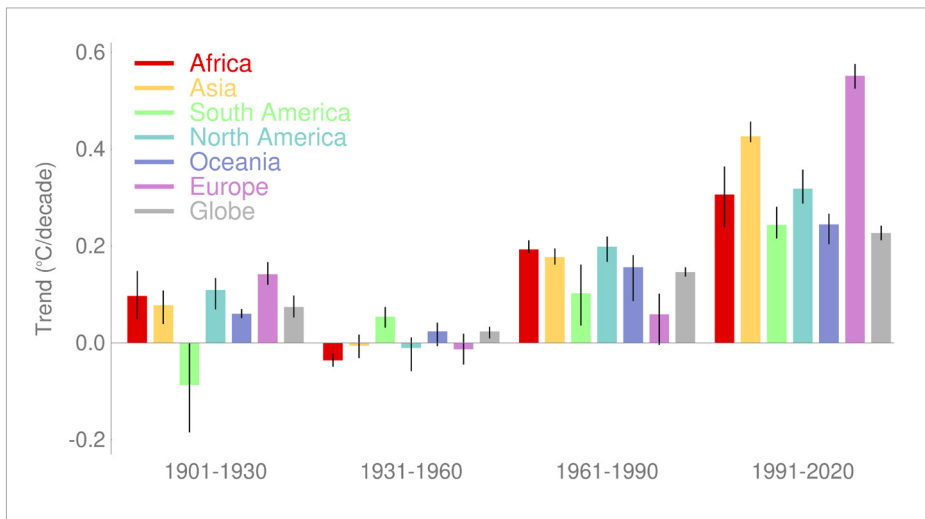


**Figure 4.** Trends in mean surface air temperature for the six WMO Regions and the global mean (°C) over four sub-periods using the six data sets (see Figure 1). The bars indicate the trend in the mean of the data sets. The black lines indicate the range between the largest and the smallest trends in the individual data sets.

## PRECIPITATION

Precipitation is a key climate parameter, closely related to indispensable resources for human activities, such as water for drinking, domestic purposes, agriculture and hydropower. It also drives major climatic events such as droughts and floods. In 2021, the largest relative precipitation deficit in the region was observed in West Asia, including, in particular, the Islamic Republic of Iran, Iraq, Afghanistan and the Arabian Peninsula. In general, South-West Asia and eastern Siberia received less than usual annual precipitation amounts (Figure 5). The largest absolute precipitation excesses, with reference to the 1981–2010 climate normal, were observed along the west coasts of India and Myanmar, in the eastern Himalayas and on the North China Plain. Abnormally high annual precipitation totals were detected in South and South-East Asia, eastern China and the West Siberian Plain.

Based on time series analyses of the area-mean annual precipitation totals from the Global Precipitation Climatology Centre (GPCC) data, 2021 was the fifth year in a row with less than normal (1981–2010) precipitation in the Western Asian steppe (the region spanning 45°E–80°E, 40°N–55°N). In the South-West Asia regions relying on winter precipitation, annual amounts were below normal in 2021, after three years with above-normal amounts. The year 2021 was the fourth consecutive year with above-normal precipitation in the Eastern Asian steppe (the region spanning 90°E–120°E, 40°N–55°N). The South Asian Monsoon region received above-normal rain amounts for the second year in a row, whereas the East Asian Monsoon brought, for the seventh consecutive year, more rain than the normal value.

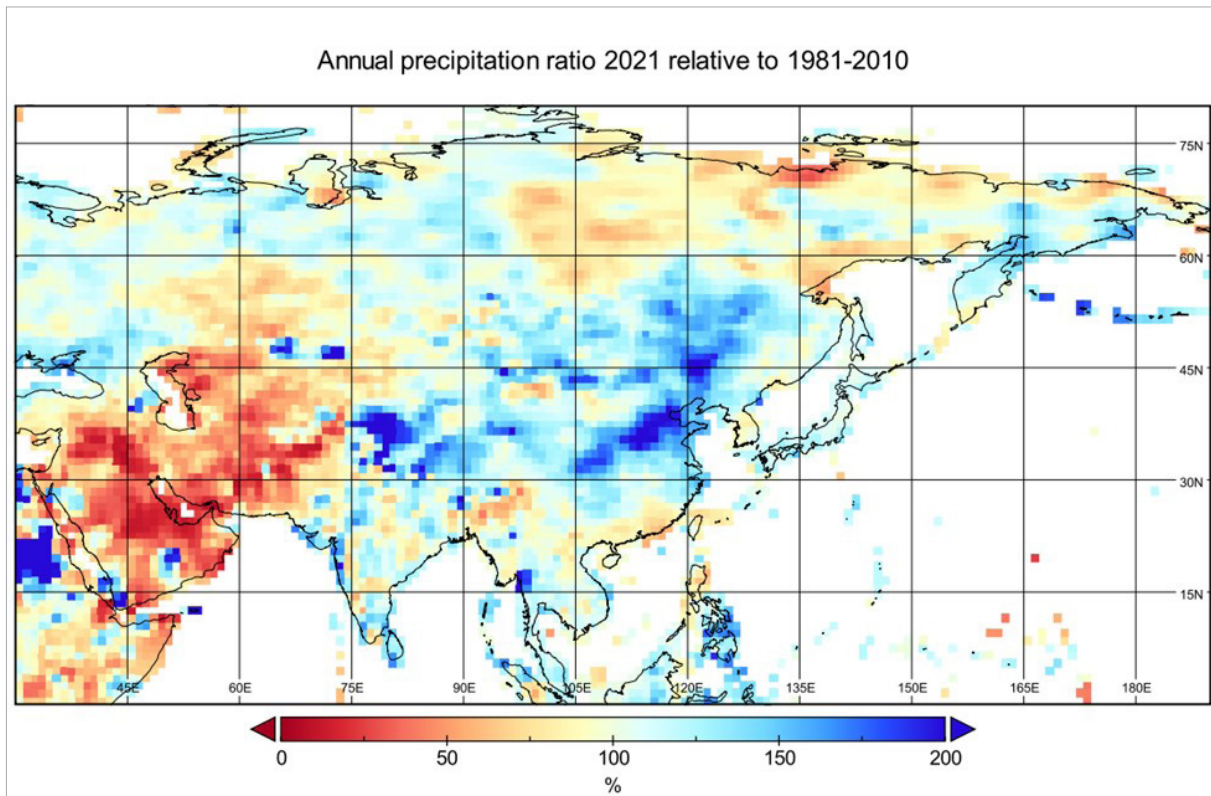


**Figure 5.** Precipitation anomalies for 2021, expressed as a percentage of the 1981–2010 average.

*Source:* Global Precipitation Climatology Centre (GPCC), Deutscher Wetterdienst, Germany

# CRYOSPHERE

## ARCTIC SEA ICE

Sea-ice extent is a key indicator of climate variability and change in the polar regions. The presence of sea ice strongly modulates surface ocean waves and the air-sea exchanges of heat, momentum, moisture and gases, shaping not only the regional climate but also the global climate.

According to the Consensus Statement of the 7th session of the Arctic Climate Forum,<sup>6,7</sup> the maximum winter sea-ice extent was reached on 11 March 2021 with a value of approximately 15 million km<sup>2</sup>, being the seventh lowest since 1979. Negative anomalies of ocean heat content in the upper 15 metres of the ocean in June 2021 and further into summer slowed ice melt in the East Siberian and Chukchi Seas. The slow melt was reinforced by near-to- or below-average air temperatures during the boreal summer across a wide area of the Arctic Ocean.<sup>8</sup> At the end of the boreal summer, the minimum sea-ice extent was reached on 12 September 2021, with a value of approximately 4.8 million km<sup>2</sup>, which is 0.9 million km<sup>2</sup> above the 2020 minimum and the twelfth lowest minimum sea-ice extent since 1979. The northern sea route was not consistently ice-free during the 2021 boreal summer.

## GLACIERS

Glacier ice mass is sensitive to changes in regional temperature, precipitation and surface radiation. As glaciers melt due to climate change, they impact global sea level, regional water cycles and local hazard occurrences. High-Mountain Asia is the high-elevation area centred on the Tibetan Plateau, and contains the largest volume of ice outside of the polar regions, with glaciers covering an area of approximately 100 000 km<sup>2</sup>. Over the last decades, most of these glaciers have been retreating, with the equilibrium line altitudes gradually rising.<sup>9,10</sup>

In the past 40 years, five glaciers (Figure 6) with long-term observations in the High-Mountain Asia region recorded significant mass losses, with an accelerating trend in the twenty-first century. In particular, the Parlung No. 94 Glacier in the south-eastern Tibetan Plateau (indicated in Figure 6 by a red line, and observed since 2006) shows a larger cumulative mass loss than the average for global reference glaciers (indicated in Figure 6 by a grey line) during the period 1980–2021.

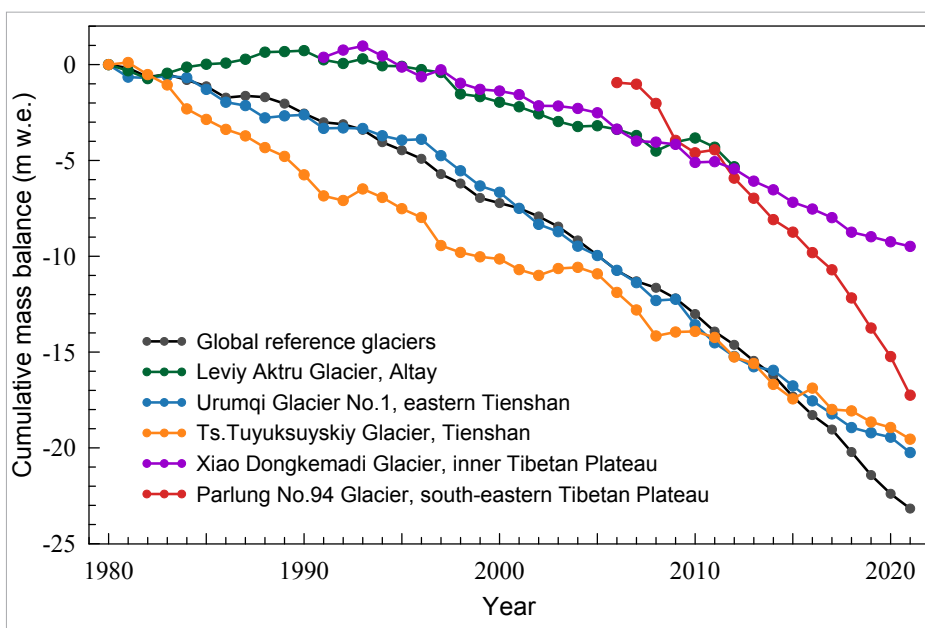


**Figure 6.** Cumulative mass balance (in metres water equivalent (m w.e.)) of five reference glaciers in the High-Mountain Asia region and the average loss of global reference glaciers. *Source:* Data for the Global reference glaciers (grey), Levy Aktru Glacier (green) and Ts. Tuyuksuyskiy Glacier (orange) are from the World Glacier Monitoring Service (WGMS).<sup>11</sup> Data for the Urumqi Glacier No. 1 (blue), Xiao Dongkemadi Glacier (purple), and Parlung No. 94 Glacier (red) are from the Chinese Academy of Sciences (CAS).<sup>12</sup>

For the glaciological year 2020/2021, preliminary data available from glaciers observed in High-Mountain Asia show a clear regional heterogeneity in mass changes (Figure 7). Most glaciers in the High-Mountain Asia region, particularly in the south-eastern Tibetan Plateau, eastern Himalayas and Pamir Alai, suffered intense mass losses as the result of exceptionally warm and dry conditions in 2021. For example, the mass balance for Parlung No. 94 in the south-eastern Tibetan Plateau reached around  $-2.0$  m w.e. in 2020/2021. The glaciological year 2020/2021 is one of the two strongest years of ablation on observation record, close to 2009. However, a portion of the glaciers in western Tianshan (in Kyrgyzstan) and the middle Himalayas (in Nepal) were close to balanced-budget conditions (meaning a small gain or loss of ice).

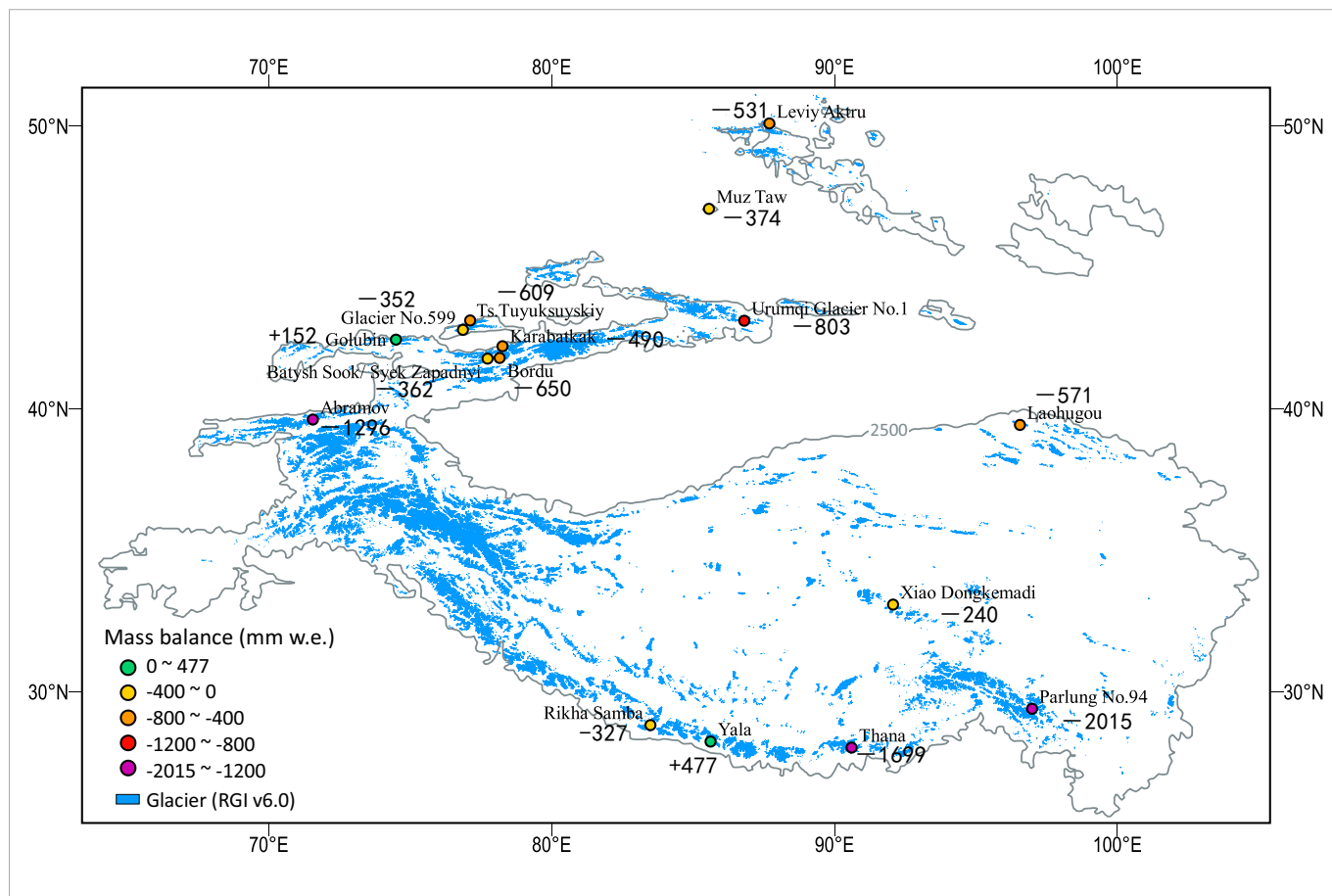


**Figure 7.** Preliminary estimations of 2020/2021 mass balance of glaciers in the High-Mountain Asia region. The area indicated by grey contours are 2500 metres above sea level. Note: Snow cover extent for the region is depicted in Figure 10. Source: WMO Third Pole Regional Climate Centre Network (TPRCC-Network) and WGMS; the original investigators are from Bhutan, China, Kazakhstan, Kyrgyzstan, Nepal and the Russian Federation.

## PERMAFROST

Permafrost is soil that continuously remains below 0 °C for two or more years, and is a distinctive feature of high-latitude environments. For example, permafrost occupies about 1 000 000 km<sup>2</sup> in the Russian Federation.<sup>13</sup> It is characterized by two parameters: mean annual soil temperature at the top of the permafrost, and thickness of the uppermost layer the seasonally thawing soil, which is defined as Active Layer Thickness (ALT). According to monitoring carried out by the Russian Federal Service for Hydrometeorology and Environmental Monitoring (RosHydroMet) in 2021,<sup>14</sup> the ALT decreased at many sites in western Siberia in 2021, due to colder conditions in Siberia in the boreal winter of 2020/21 compared to the winter of 2019/20. On the other hand, trends in ALT (Figure 8) at almost all other sites remain positive, which indicates a steady trend towards an increase in the depth of permafrost thaw in the twenty-first century. In terms of soil temperature, in most of North Asia, positive anomalies prevail in the entire soil layer up to 320 cm, compared to the 2007–2021 average (up to +2 °C). The largest and statistically significant increase in the minimum soil temperature, penetrating to the lower depth of 320 cm, was observed in the northern parts of Siberia.

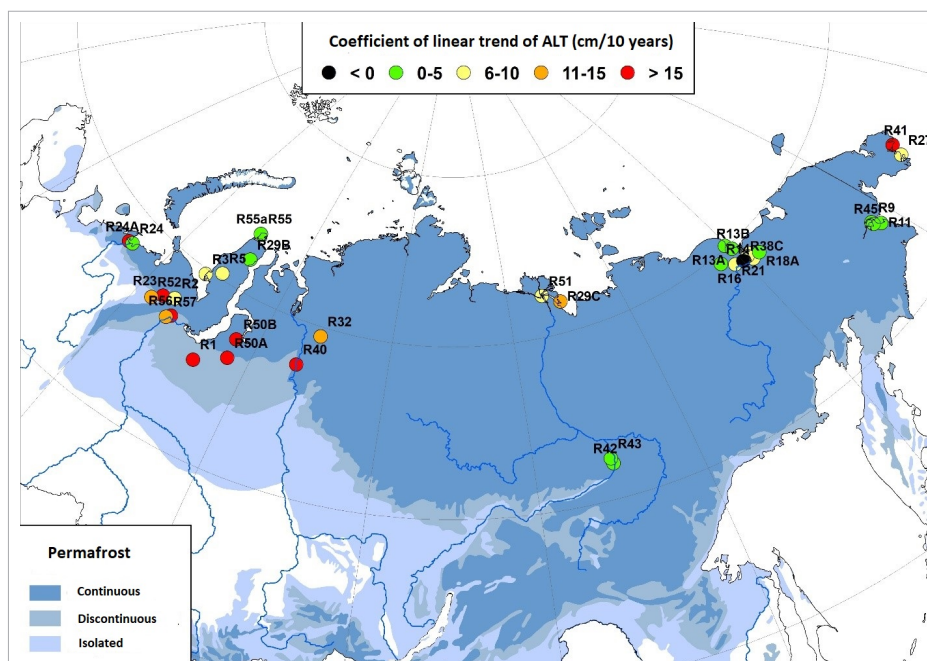


**Figure 8.** Long-term trend of the thickness of the uppermost layer of seasonally thawing soil (active layer thickness, ALT in cm per 10 years) for the period 1976–2021. Permafrost is classified by coverage into continuous (90%), discontinuous (50–90%) and sporadic (10–50%) zones, and isolated patches (10%), depending on area continuity.

## SNOW COVER

Snow cover plays an important role in the feedback mechanisms in the climate system (such as albedo,<sup>15</sup> run-off, soil moisture and vegetation). Hence, it is a crucial variable for monitoring climate change. In the past 25 years, the boreal spring (March to May) snow cover extent (SCE) over Asia has exhibited decadal-scale variations with a decreasing tendency, though the tendency is not statistically significant. The SCE in spring was dominated by positive anomalies prior to 2006, and by negative anomalies thereafter. In the spring of 2021, SCE in Asia was about 14.15 million km<sup>2</sup>, which is 0.53 million km<sup>2</sup> less than the 1998–2020 average (Figure 9).

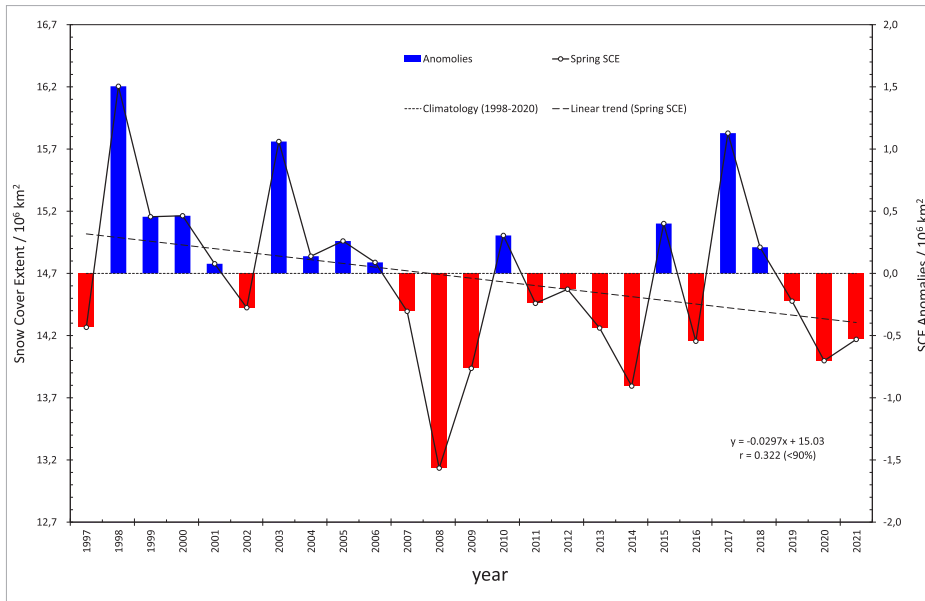


**Figure 9.** SCE in Asia (left axis) and anomalies in blue and red (right axis) in the boreal spring, 1997–2021. The dotted line denotes the climatology mean 1998–2020. The dashed line denotes the linear trend 1997–2021. The Interactive Multisensor Snow and Ice Mapping System and data from the National Snow and Ice Data Center (<https://nsidc.org/home>) were used.

Compared to the average over the period 1998–2020, SCE in the spring of 2021 was below normal in a wide-ranging part of Asia except in the latitudes around 40°N (in the western Tianshan and western Kunlun Mountains) and between 50°N and 60°N, where the SCE in spring was mostly 50 to 60 km<sup>2</sup> above normal, and locally 120 km<sup>2</sup> above normal (Figure 10).

The duration of snow cover in northern Asia for the boreal winter of 2020/2021 was significantly below normal.<sup>16</sup> In the polar regions, the number of days of snow coverage was at a record low. Conversely, the maximum average snow depth in Siberia was significantly higher than the climatological normal, falling into the top ten values on record.

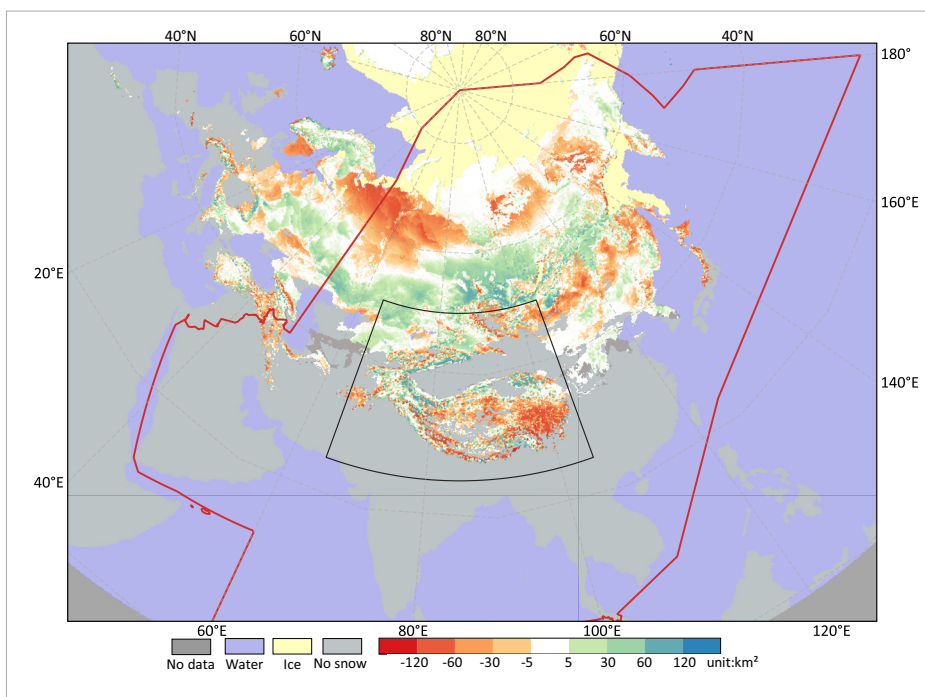


**Figure 10.** Anomalies of mean SCE in the boreal spring of 2021, relative to the 1998–2020 average. Note: The red line delimits the geographical area for which the Asian mean SCE was calculated, as shown in Figure 9. The black line delimits the High-Mountain Asia region displayed in Figure 7. The Interactive Multisensor Snow and Ice Mapping System and data from the National Snow and Ice Data Center (<https://nsidc.org/home>) were used.

## SEA-SURFACE TEMPERATURE

Sea-surface temperature (SST) is an important physical indicator for Earth’s climate system. Changes in SST play a critical role in the coupling between the ocean and the atmosphere, as they can trigger the transfer of energy, momentum and gases between the two Earth system components.<sup>17</sup>

The rate of SST warming varies according to region, with slight cooling in some regions in recent decades. The ocean area of WMO Regional Association II shows an overall sea-surface warming trend (Figure 11) at rates of more than 0.4 °C per decade in the areas of the Kuroshio Current system, the Arabian Sea, the southern Barents and Kara Seas and the south-eastern Laptev Sea. This is about three times faster than the global sea-surface warming rate of 0.16 +/- 0.01 °C per decade.<sup>18</sup> In 2021, the area-averaged SST anomalies reached near-record values in the north-west Pacific Ocean (area 2 in Figure 11) (> 0.6 °C), whereas the values in the Arctic area and Indian Ocean (areas 1 and 3 in Figure 11) lie below the record values reached in 2020. The Barents Sea is identified as a climate change hotspot,<sup>19</sup> and a gateway for the recent Arctic amplification.<sup>20</sup> Sea-surface warming in this area also has a major impact on the observed sea-ice loss<sup>21</sup> – a feedback mechanism which in turn enhances ocean warming.<sup>22,23</sup>

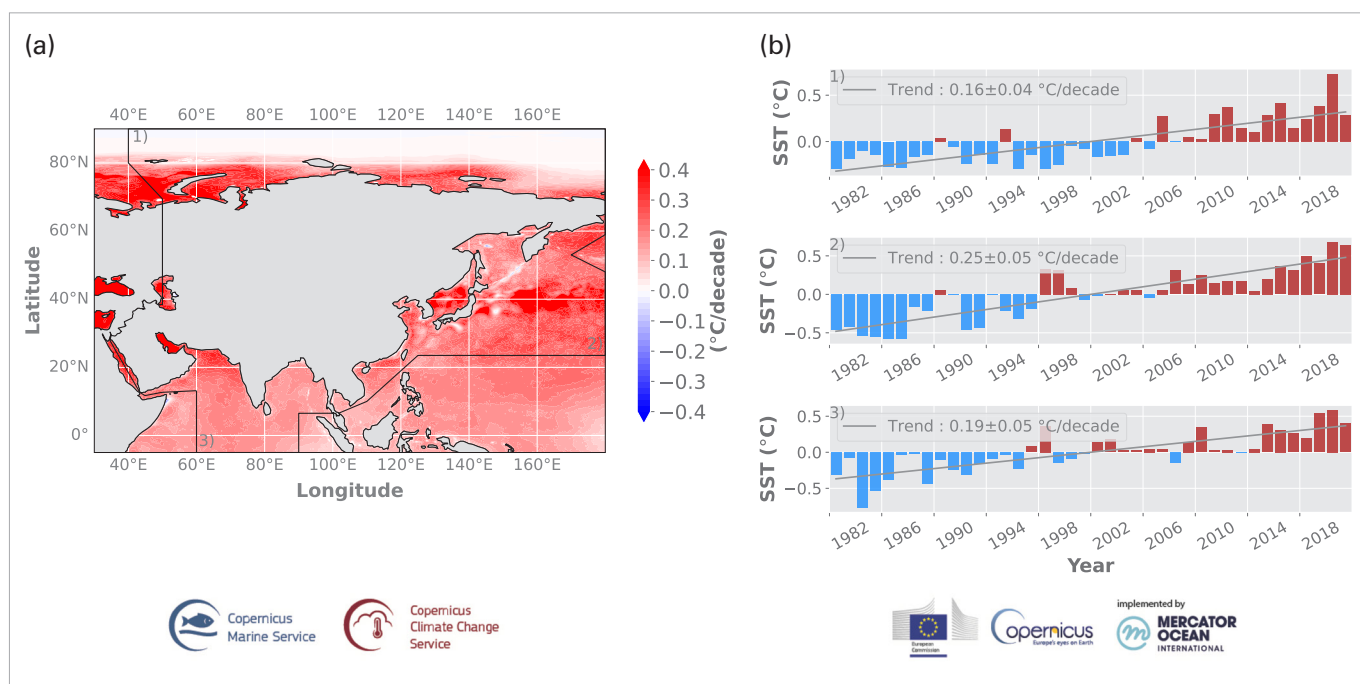


**Figure 11.** (a) Sea-surface temperature trend (in °C per decade) over the period 1982–2021, derived from the remote-sensing product downloaded from <https://marine.copernicus.eu/> (product name: SST\_GLO\_SST\_L4\_REP\_OBSERVATIONS\_010\_024). (b) Area-averaged time series of sea-surface temperature anomalies relative to the 1982–2021 reference period (in °C) within three areas of the WMO Regional Association II, as bordered by the black line in panel (a), that is: 1) for the Arctic area north of 60°N; 2) for the north-west Pacific Ocean area; and 3) for the Indian Ocean area. The linear trend over the full period is indicated as a grey line.

## OCEAN HEAT CONTENT

Due to emissions of heat-trapping gases resulting from human activities, the global ocean has warmed. It has taken up more than 90% of the excess heat in the climate system, making climate change irreversible on centennial to millennial timescales.<sup>24</sup> Ocean warming contributes about 40% of the observed global mean sea-level rise,<sup>25</sup> and is altering ocean currents. It also indirectly alters storm tracks,<sup>26</sup> increasing ocean stratification,<sup>27</sup> and can lead to changes in marine ecosystems.<sup>28</sup>

Most of the regions in the WMO Regional Association II area (Asia) show upper-ocean (0–700 m) warming since 1993 (the start date of satellite altimetry records). Warming is particularly strong in the Arabian Sea and in the Kuroshio Current system, at rates exceeding  $2 \text{ W/m}^2$  – more than three times faster than the global mean upper-ocean warming rate of  $0.6 \text{ W/m}^2$  over a similar period (Figure 12(a)). In 2021, the area-averaged ocean heat content continued to reach record values ( $> 4 \times 10^{28} \text{ J/m}^2$ ) in the Pacific and the Indian ocean components of WMO Regional Association II (Figure 12(b)). These areas are specifically characterized by a rapid subsurface ocean warming rate, currently measured at a rate of  $0.8 \pm 0.3 \text{ W/m}^2$  between 1993–2021, which is in the range of the global ocean warming rate. The warming in the area north of  $60^\circ\text{N}$  is not significant and is dominated by strong year-to-year variations. However, the result may be affected by the 300 m bathymetry product limitation.

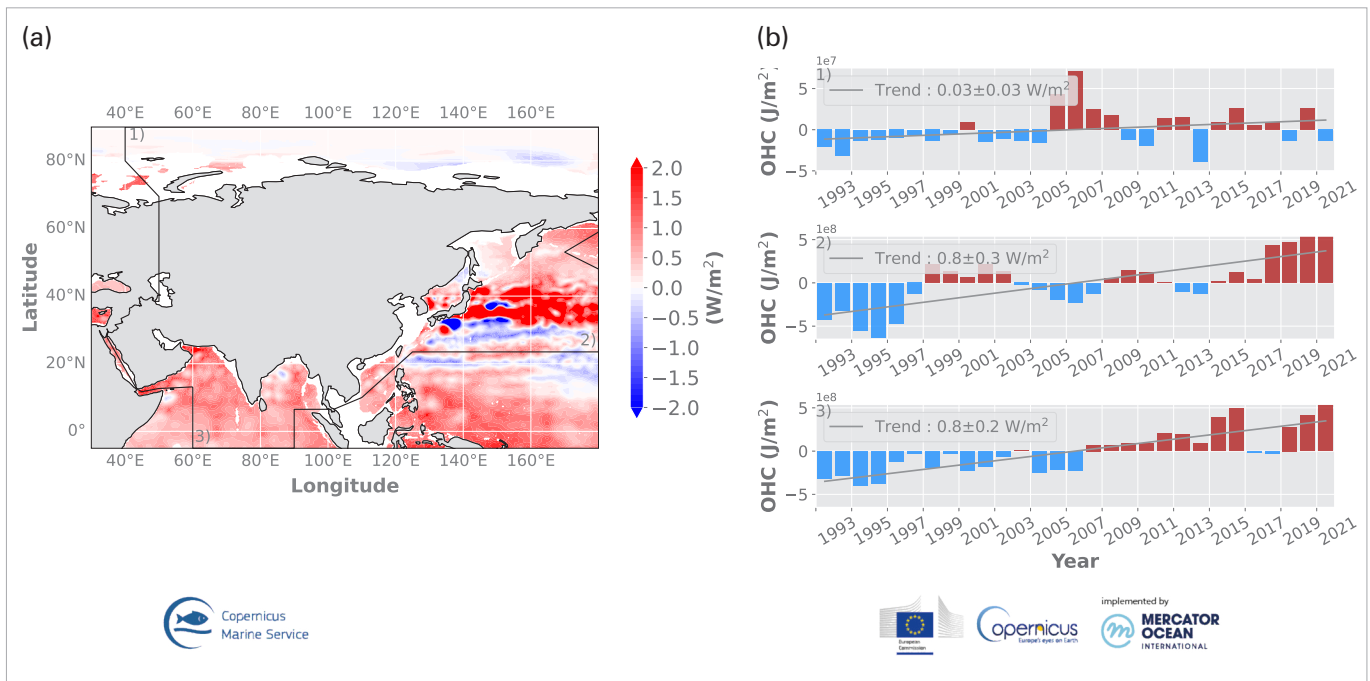


**Figure 12.** (a) Ocean heat content trend (units: watts per square metre,  $\text{W/m}^2$ ) over the period 1993–2021, integrated from the surface down to a 700 m depth, and derived from the in situ-based product downloaded from <https://marine.copernicus.eu/> (product name: MULTI-OBS\_GLO\_PHY\_TSUV\_3D\_MYNRT\_015\_012). Ocean warming rates in areas shallower than 300 m have been masked in grey due to product limitations. (b) Area-averaged time series of ocean heat content anomalies relative to the 1993–2021 reference period (units: joule per square metre,  $\text{J/m}^2$ ) within three areas of the WMO Regional Association II as bordered by the black line in panel (a), that is: 1) and 2) for north-west Pacific and Indian Ocean areas, respectively; and 3) for the Arctic area north of  $60^\circ\text{N}$ . The linear trend over the full period is indicated as a grey line.

## SEA LEVEL

In 2021, the global average sea level continued to rise in response to ocean warming (via thermal expansion) and the melting of glaciers, ice caps and ice sheets. However, the rate of rise is not the same everywhere. The rates of sea-level change in the Indian Ocean, western tropical Pacific region, south Pacific region and northern mid-latitude Pacific region are slightly faster than the global mean of 3.3 mm per year (Figure 13; Table 1). On the other hand, along the Asian coasts of the Pacific Ocean, the rate of rise is close to the global average. The observed non-uniform regional trends in sea level are essentially due to non-uniform ocean thermal expansion in conjunction with salinity changes in some regions.<sup>29,30</sup> Table 1 summarizes the coastal sea-level trends over the period from January 1993 to December 2021 in six subregions (highlighted by the numbered boxes shown in Figure 13).

**Table 1.** Rate of area-averaged sea-level change over the 1993–2021 satellite measurement period. Subregions are defined in Figure 13.

Subregion number	Area	Trends in rate of sea-level rise (in mm per year)
1	North-West Indian Ocean	$3.78 \pm 0.1$
2	North-East Indian Ocean	$3.84 \pm 0.1$
3	South-East Indian Ocean	$3.79 \pm 0.1$
4	Sea off the eastern coast of Australia	$3.65 \pm 0.1$
5	Western tropical Pacific region	$3.94 \pm 0.1$
6	North-West Pacific region	$3.59 \pm 0.1$

Though the regional sea-level time series (not shown) display strong interannual variability, mostly driven by the El Niño–Southern Oscillation (ENSO), especially in the eastern Indian Ocean and tropical Pacific Ocean, sea levels in all six subregions show statistically significant rising trends at rates generally slightly above the global mean rate, as they approach 4 mm per year.

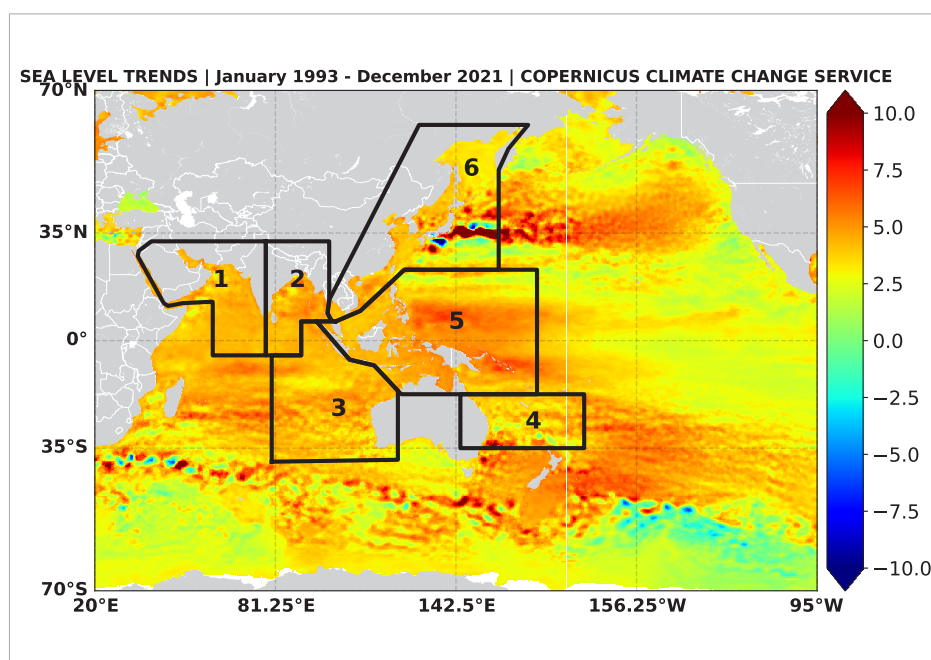


**Figure 13.** Spatial patterns in sea-level trends observed by altimeter satellites over the period 1993–2021. Boxes represent subregions where the rates of area-averaged sea-level change are provided in Table 1. Source: Copernicus Climate Change Service, C3S: <https://climate.copernicus.eu/sea-level>

## MAJOR CLIMATE DRIVERS

There are many modes of natural variability, often referred to as climate patterns or climate modes, which affect weather at timescales ranging from days to months or even decades. Surface temperatures change relatively slowly over the ocean, so recurring sea-surface temperature (SST) patterns can be used to understand and, in some cases, predict the more rapidly changing patterns of weather over land on seasonal timescales. Similarly, albeit at a faster rate, known pressure changes in the atmosphere can help explain certain regional weather patterns.

### EL NIÑO–SOUTHERN OSCILLATION

The El Niño–Southern Oscillation (ENSO) is one of the most important drivers of year-to-year variability in weather patterns in Asia.<sup>31</sup> La Niña, as the negative phase of ENSO, characterized by below-average SSTs in the central and eastern Pacific Ocean and strengthening of the trade winds, typically has a cooling influence on global temperatures.

La Niña conditions emerged in mid-2020 and peaked in the boreal autumn at moderate strength, with average sea-surface temperatures 1.3 °C below the 1991–2020 normal in the Niño 3.4 region (5°N–5°S, 120°W–170°W). Through the first half of 2021, La Niña weakened and reached an ENSO-neutral state (SSTs in the central and eastern Pacific Ocean within  $\pm 0.5$  °C of normal) from May to August 2021. However, SSTs cooled after mid-2021 and La Niña re-emerged in October, reaching moderate strength in December (Figure 14). The atmospheric circulation responded to the anomalous oceanic conditions and induced convective activity that led to anomalous climate conditions over Asia. The wetter conditions and cold anomaly around the Indochinese Peninsula in April were signs of a typical La Niña influence. A series of heavy snowfall events on the Sea of Japan side of Japan after the middle of December 2020 until early January 2021 was also attributable to the anomalous convective activity over Indonesia associated with the prevailing La Niña conditions.<sup>32</sup>

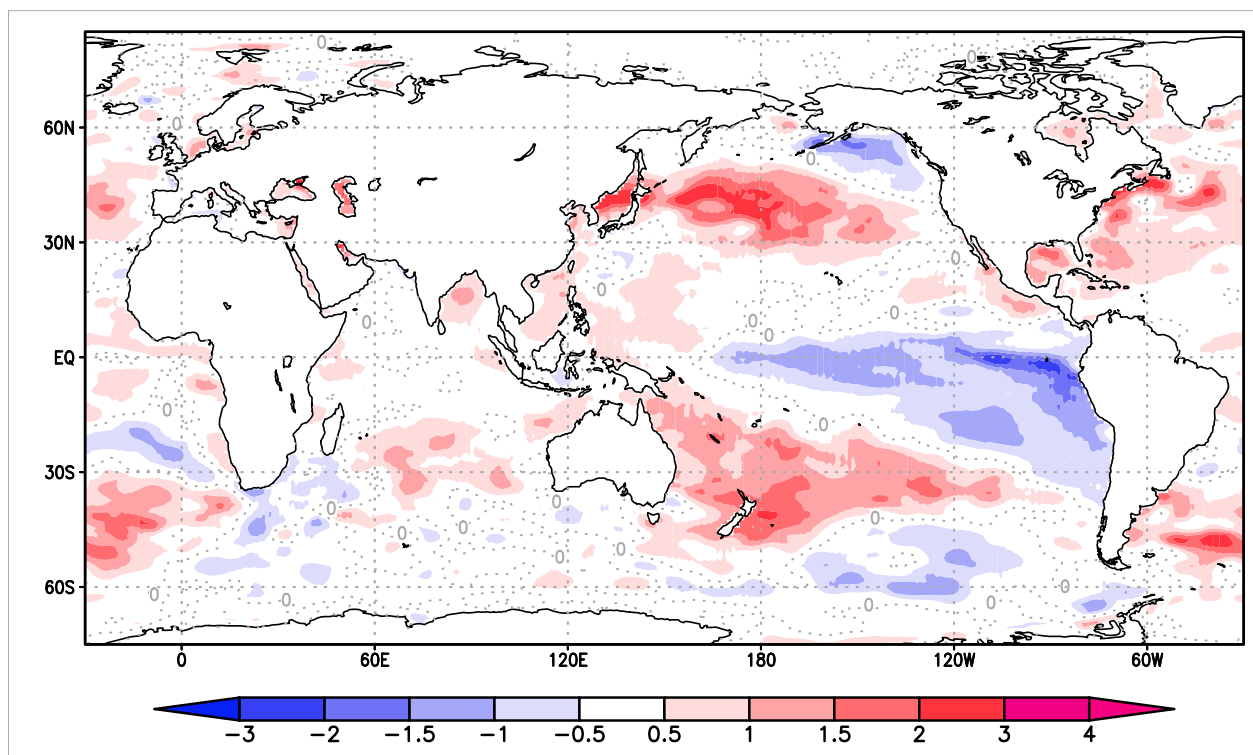


**Figure 14.** Global SST anomalies (°C) in December 2021. Anomalies are defined as deviations from the 1981–2010 mean.  
Source: Tokyo Climate Center, Japan Meteorological Agency

## INDIAN OCEAN DIPOLE

The Indian Ocean Dipole (IOD) is an inherent and major mode of climate variability over the Indian Ocean. It is characterized by SST anomalies and associated convective anomalies with opposite signs in the eastern and western tropical Indian Ocean. A negative IOD (which is characterized on the one hand by above-normal SSTs and enhanced convection in the south-eastern part of the tropical Indian Ocean, and on the other hand by above-normal SSTs in the western part), developed during July 2021 and returned within the neutral range by the end of the year, although tending towards the negative side. In association with this negative IOD, the centre of convective activities was shifted southward, and convection was suppressed over the Asian summer monsoon region. The drier conditions on the Indochinese Peninsula in summer and the rainfall deficit over India, especially in the month of August, were linked to this convective activity, and therefore these could be considered an effect of the negative IOD conditions. This anomalous convection also likely brought about a southward shift of the subtropical jet stream, which is considered to have prepared favourable conditions for updraft and resulting heavy rainfall over western and eastern Japan in August (see also [Heavy precipitation and flooding](#)).

## ARCTIC OSCILLATION AND WINTER MONSOON

The Arctic Oscillation (AO) is a large-scale atmospheric pattern that influences weather throughout the northern hemisphere. The AO index was negative for most of the boreal winter of 2020/2021, with the lowest values in February. It was characterized by higher-than-normal surface pressure over the polar region and lower-than-normal pressure over the surrounding southern regions. Consequently, the Siberian High was strong in December and January, leading to colder-than-normal conditions over East Asia (see also [Impact on the economy](#)).

## ASIAN MONSOON

The Asian summer monsoon is one of the world's prominent monsoon systems. It is also a key driver of the seasonal changes in atmospheric circulation and precipitation (dry and wet seasons) over several countries in South and East Asia. Precipitation associated with the Asian summer monsoon is a key source of fresh water in those regions.

In 2021, the East Asia summer monsoon was stronger than normal and the Meiyu/Baiu/Changma<sup>33</sup> season, which started later and ended earlier than the 1991–2020 normal, was shorter overall. The south-west monsoon set in over the north Andaman Sea on 21 May and progressed northward, setting in over the southern tip of India on 3 June (the normal date is 1 June).<sup>34</sup> Though large intraseasonal variations were observed, the south-west monsoon season rainfall over India was close to normal, as rainfall during the season was 99% of its climatological normal for the 1961–2010 period (Figure 15). Bangladesh, Pakistan and Sri Lanka reported much-above-normal rainfall during the summer monsoon season.

The north-east monsoon, which contributes 30% to 50% of the annual rainfall over southern peninsular India and Sri Lanka as a whole, set in over southern peninsular India during October and over Sri Lanka in late November. The seasonal rainfall over southern peninsular India during the north-east monsoon was exceptionally above normal (171% of the long-term average) and was the highest (579.1 mm) since 1901. During the season, many low-pressure systems (wind speed less than 17 knots) formed in the south and adjoining the central Bay of Bengal. These systems moved in a westerly/north-westerly direction and caused large amounts of rainfall.

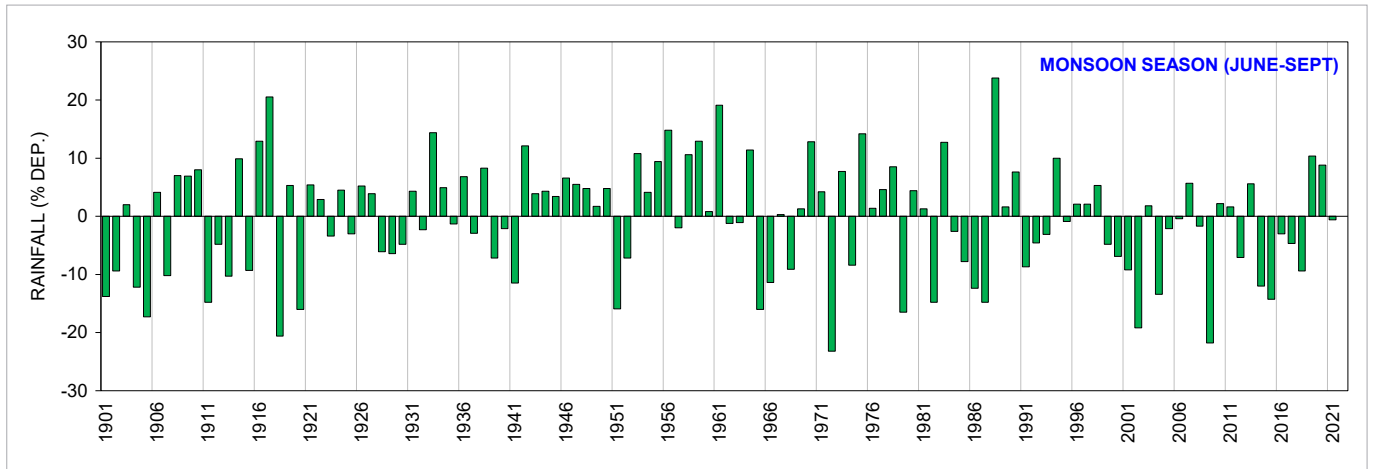


**Figure 15.** Time series of area-weighted rainfall anomalies over India (representative of South Asia) in the summer monsoon season (June to September) for the period 1901–2021. Anomalies are defined as a departure from the 1961–2010 average (%DEP). *Source:* Regional Climate Centre (RCC), Pune, India

### ATMOSPHERIC RIVERS OVER ASIA

Atmospheric rivers (ARs) are long, narrow (up to a few hundred km wide), shallow (up to a few km deep) and transient corridors of strong horizontal water vapour transport that are typically associated with a low-level jet stream ahead of the cold front of an extratropical cyclone. ARs are most active over mid-latitude oceans and play a critical role in the global Equator-to-Pole water vapour transport. Regionally, the intense water vapour fluxes in ARs often cause heavy precipitation and flooding, and play a key role in shaping water resources over the land in the vicinity of AR landfalls.<sup>35,36,37,38,39,40</sup> The AR frequency for the period from 1979 to 2021 (Figure 16) derived from the ERA5 reanalysis data,<sup>41</sup> shows positive trends over the East Asia and South Asia regions. The regions experienced above-average AR frequency in 2021.

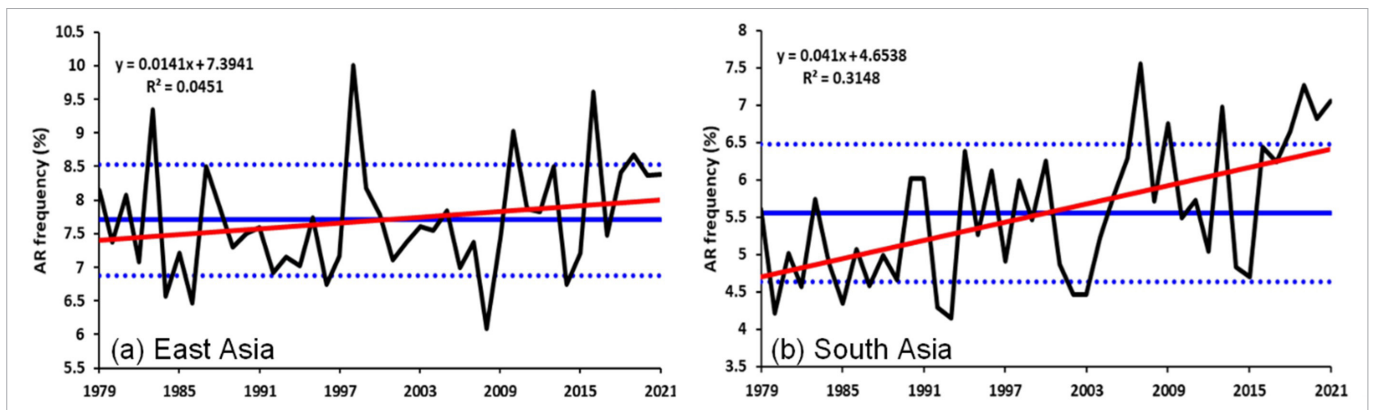


**Figure 16.** The annual AR frequency over the (a) East Asia (111°E–150°E, 21°N–54°N) and (b) South Asia (60°E–109.5°E, 6°N–30°N) regions for the period from 1979 to 2021, obtained by applying the Park et al. (2021) AR detection scheme to the ERA5 reanalysis data. The solid blue line indicates the climatological mean and the dashed blue line indicates the range for a 95% significance level. The red solid line is the linear trend.

# Extreme events

## TROPICAL CYCLONES

### WESTERN NORTH PACIFIC OCEAN AND SOUTH CHINA SEA

In 2021, a total of 22 tropical cyclones (TCs) with maximum sustained wind speeds of  $\geq 34$  knots formed over the western North Pacific Ocean and the South China Sea, which was below the normal of 26 TCs (1981–2010 average).<sup>42</sup> During August and September, when the number of TC formations is generally at its highest, convection was largely inactive over the ocean areas where many TCs are formed climatologically. In total, 8 TC formations occurred during this period, which is below the normal of 11.

Typhoon *In-fa* affected Japan and mainland China with torrential rain, strong winds and high waves, resulting in flooding over wide areas. It made landfall over the coast of central China and brought 700 to 900 mm of precipitation in the northern part of Zhejiang Province from 22 July to 1 August. Typhoon *Chanthu*, the second strongest TC of the 22 TCs in 2021, affected the Republic of Korea and Japan. From 15 to 17 September, accumulated precipitation of 544 mm was recorded on Mount Halla on Jeju Island. Tropical Storm *Dianmu* hit Viet Nam, then weakened and moved into Lao People's Democratic Republic and Thailand, resulting in heavy rainfall, flooding and landslides in these countries. In Thailand, *Dianmu* brought daily rainfall of 362 mm in upper Thailand in Phaisali, in Nakhon Sawan Province, on 25 September. The third strongest TC of the 22 TCs in 2021 was Typhoon *Rai*, which formed in December. After it reached its first peak intensity and subsequently passed over the central part of the Philippines, it reached its second peak intensity with maximum sustained winds of 105 knots over the South China Sea, bringing floods to Viet Nam.

### NORTH INDIAN OCEAN

During 2021, five cyclonic storms with maximum sustained wind speeds of  $\geq 34$  knots formed over the North Indian Ocean. The most devastating was Extremely Severe Cyclonic Storm *Tauktae* (14 to 19 May) which formed in the pre-monsoon season over the Arabian Sea, and crossed the Saurashtra coast on 17 May, claiming more than 140 lives across western India. Cyclone *Shaheen* formed from the remains of Cyclone *Gulab* in late September. Cyclone *Shaheen* made landfall on 3 October on the northern Oman coast. Al-Khaburah and Al-Suwaiq, Oman, recorded the highest rainfall, with 369 mm and 300 mm on 2 and 4 October respectively (see also [Affected population and damage](#)). The United Arab Emirates experienced light to moderate rains, particularly in the eastern and south-eastern parts of the country. The wave height over the eastern coast of the United Arab Emirates significantly increased during these days, due to fresh to strong north-easterly winds.

## HEAVY PRECIPITATION AND FLOODING

With regards to extremes based on daily precipitation totals, the highest five-day precipitation amounts were measured in regions influenced by the South and East Asian monsoons and tropical storms, such as most mountain ranges and coastal regions in South and South-East Asia. The highest totals were observed in the South China Highlands, and central and north China, as shown by the darkest blue colour in Figure 17. In July, heavy rainfall was recorded in central and north China, with maximum cumulative precipitation records observed at 26 stations, including Zhengzhou in Henan Province (851 mm). Among these extreme events, Zhengzhou observed a maximum *daily* precipitation total of 624.1 mm, close to its *annual* normal of 641 mm (see also [Impact on the economy](#)). In August, active stationary fronts with moist air brought record-breaking monthly precipitation amounts to western Japan.

During the monsoon season, some heavy rainfall, associated floods and landslide events brought casualties in Nepal (see also [Agriculture and food security](#)) and Bhutan. Mahabaleshwar station in India recorded 480.0 mm of rainfall on 22 July and 594.4 mm on 23 July (see also [Affected population and damage](#)). Record-breaking torrential rainfall was also observed in some of the South-East Asian nations. The new highest daily rainfall of 202.0 mm was recorded at Takfa agrometeorological station, in Nakhon Sawan Province, Thailand, on 25 September 2021, and more than 50 000 households were flooded.

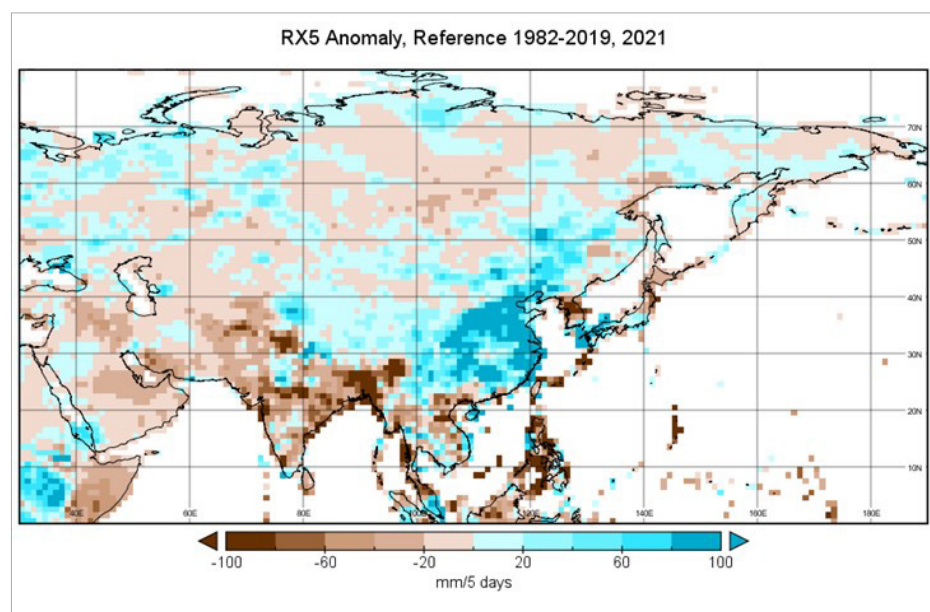


**Figure 17.** Anomalies (mm/5 days) of the highest five-day precipitation totals. Blue indicates more extreme precipitation than the long-term mean, and brown indicates less extreme precipitation than the long-term mean. Note: The climatology period used here is the full length of the global daily precipitation data set. *Source:* Global Precipitation Climatology Centre (GPCC), Deutscher Wetterdienst, Germany.

## DROUGHTS

Significant droughts occurred during 2021 in several countries including in West Asia, Central Asia, South Asia and South-East Asia, due to large precipitation deficits. Almost half the average precipitation fell during January and February in the Islamic Republic of Iran, leading to significant droughts, reduced streamflow in rivers and reduced water availability for irrigation. Pakistan had its third-driest February and fifth-driest January–March on record. Drier conditions in the region, such as in Pakistan, the Islamic Republic of Iran and Iraq, continued in the boreal summer of 2021.<sup>43,44,45</sup> During the 2020/2021 winter, moderate to severe meteorological droughts in Jiangnan and south China developed rapidly due to high temperatures and scarce precipitation: most areas were 50%–80% below normal, with Hunan and Guangxi recording the lowest precipitation in the same period since 1961, and with Guangdong recording the second lowest (see also [Agriculture and food security](#)).

## HEATWAVES AND WILDFIRES

Temperatures over the Asian part of the Russian Federation were exceptionally high in the boreal summer, with the warmest August and the warmest summer on record since 1936. Prolonged heatwaves caused intense and extensive forest fires and wildfires in Siberia, especially in the Yakutia region (with approximately 2 300 fires burning about 8.9 million hectares in total by the end of summer).<sup>46</sup> In Japan, seasonal mean temperatures for summer were significantly above normal in the northern part of the country, and monthly mean temperatures for July were the highest on record over the Hokkaido region. These record high temperatures from Siberia to northern Japan were associated with persistent anti-cyclonic circulation anomalies in the troposphere over these regions. In China, the July monthly mean temperature was the second highest for a month of July since 1961 (when records began), and the September monthly mean

was the highest for a month of September since 1961. Hong Kong, China, experienced its hottest March, May and September on record in 2021. With much hotter-than-normal weather from May to mid-October, 61 hot nights (daily minimum temperature  $\geq 28.0$  °C) and 54 very hot days (daily maximum temperature  $\geq 33.0$  °C) were reported in 2021 in Hong Kong; both of these were the highest annual totals since the start of records in 1884. At Bahrain International Airport, daily maximum temperatures exceeded 40 °C on 21 consecutive days (26 July–15 August). Dammam station in Saudi Arabia recorded 51.0 °C on 13 August 2021, which was the highest maximum temperature on record in the country.

## OTHER EXTREME EVENTS

Mongolia suffered strong winds and dust storms that spread across the country from 13 to 15 March. Ten people died and more than 700 were injured. On 12 March, a dust storm also affected Saudi Arabia and Oman. Many weather stations in Saudi Arabia recorded dust storms and blowing dust. Visibility was reduced to less than 1 km at many weather stations in Saudi Arabia and to 20 metres at Bahrain International Airport, where the highest maximum wind gust speed (52 knots) for March since 1974 was recorded (see also [Affected population and damage](#)). In mid-June, another dust storm, resulting from northerly winds, entered Saudi Arabia through the western parts of the United Arab Emirates and later moved to some internal areas of the country. The region of Iraq was thought to be the origin of this dust, which spread out to reach Bahrain, Qatar and the inland portion of the United Arab Emirates.

In the boreal summer of 2021, dry conditions and severely reduced precipitation caused drying of the Hamoon Lake in the eastern part of the Islamic Republic of Iran. The northerly strong summer winds known as the "120-day wind" raised more sand than usual, and the region experienced more frequent severe dust storms than usual. A severe dust storm struck the coastal city of Karachi, Pakistan, after Tropical Cyclone *Tauktae* crossed the Indian coast.

In India in recent years, lightning accompanied by thunderstorms has been one of the biggest killers. In 2021, thunderstorms and lightning claimed around 800 lives in different parts of the country. On 12 July, more than 70 people were killed in lightning strikes in Rajasthan, Uttar Pradesh and Madhya Pradesh.

## FILLING THE GAPS IN OBSERVATION

While the evidence for climate change in the Asia region is unequivocal, the most recent Intergovernmental Panel on Climate Change (IPCC) reports show that significant gaps remain in the observation of some variables over the continent, particularly precipitation. The current gaps in global surface-based data-sharing significantly impact the quality of weather and climate information locally, regionally and globally. While some parts of the globe provide a reliable feed of these data, many others contribute only limited amounts and, in several instances, the amount of data shared is even declining.

To improve observational capabilities, in 2019 the World Meteorological Congress and its 193 member countries and territories agreed to establish the [Global Basic Observing Network](#) (GBON). GBON is a landmark agreement and offers a new approach in which the basic surface-based weather observing network is designed, defined and monitored at the global level.

To achieve sustained compliance with the GBON requirements, substantial investments, strengthened capacity and long-term resources for operation and maintenance is needed in many countries. For this purpose, the [Systematic Observations Financing Facility](#) (SOFF) was established to provide technical and financial assistance in new, more effective ways, thereby: (i) applying internationally agreed metrics to guide investments; (ii) using long-term, sustained data-sharing as a measure of success; and (iii) creating local benefits while providing a global public good.

The Global Climate Observing System (GCOS), which provides an operational framework for integrating and enhancing the observational systems of participating countries and organizations, regularly reviews the state of global climate observations and publishes reports on its findings. The latest *GCOS Status Report* (GCOS-240),<sup>1</sup> published in 2021, highlighted recent improvements in global observational capabilities and identified issues and gaps in the observing systems.

For instance, the report pointed out that the most urgent need for closing observational gaps of glaciers is in regions where glaciers dominate run-off during warm/dry seasons, such as in Central Asia. In addition, in the region with the largest glacier-covered area in Asia, the Karakoram, not a single glacier is frequently monitored. This leads to huge gaps in understanding processes, and to related high uncertainties in modelling future glacier evolution. There are also some large spatial gaps in permafrost monitoring, especially in central Siberia.

Subsurface measurements of the oceans are critical to monitor and forecast the climate system. Although the uncertainty in Earth's energy budget has been substantially decreased since 2000 with the deployment of the Argo system (which collects data from inside the world's oceans), large gaps also still exist. The decision by the Argo Steering Team to expand the Argo program to the full water column and under sea ice, including biogeochemical variables, as well as the deployment of repeated hydrography, the deployment of fixed-point and other autonomous observing platforms and their integration, all aim to address these gaps.

*The 2022 GCOS Implementation Plan* (GCOS-244)<sup>2</sup> aims to address these gaps by providing a set of high priority actions which, if undertaken, will improve global observations of the climate system and our understanding of how it is changing.

1 Global Climate Observation System (GCOS). [The Global Climate Observing System 2021: The GCOS Status Report](#) (GCOS-240); World Meteorological Organization: Geneva, 2021.

2 Global Climate Observation System (GCOS). [The 2022 GCOS Implementation Plan](#) (GCOS-244); World Meteorological Organization: Geneva, 2022.

# Climate-related impacts and risks

The impacts of climate change and increasing inequality across and within countries are undermining progress on the sustainable development agenda. In addition, extreme weather conditions and more frequent and severe disasters are causing increased food insecurity and are worsening human safety and health, forcing many communities to suffer from poverty, displacement and widening inequalities.

## AFFECTED POPULATION AND DAMAGE

In 2021, there were a total of more than 100 natural hazard events in Asia, of which over 80% were flood and storm events. These natural hazard events resulted in almost 4 000 fatalities, of which around 80% were caused by flooding. Overall, 48.3 million people were directly affected by these hazards, causing total economic damage of US\$ 35.6 billion. While floods caused the highest fatalities and economic damage, drought in the region affected the highest number of people (Figure 18).

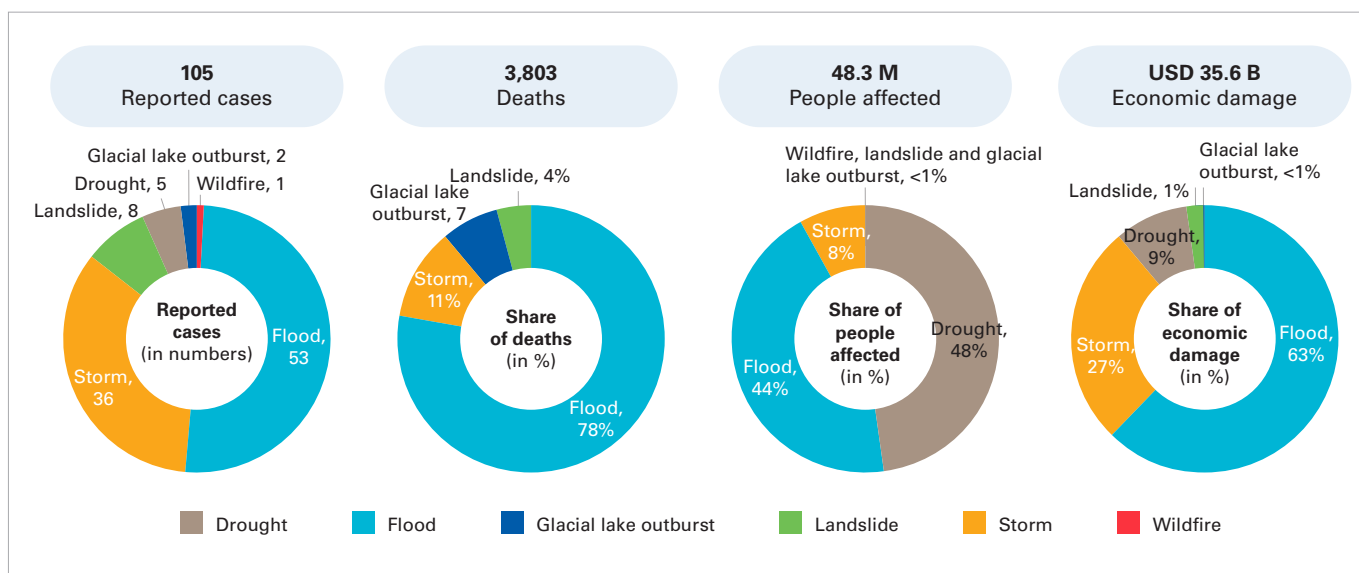


**Figure 18.** Overview of 2021 disasters in the Asia region.

Source: ESCAP calculations based on EM-DAT, accessed on 30 April 2022.

Note: The economic damages of some disaster occurrences are not presented in the diagram due to data unavailability. ESCAP – Economic and Social Commission for Asia and the Pacific; EM-DAT – Emergency Events Database.

In 2021, the disaster event with by far the greatest impact in Asia in terms of fatalities and economic damage was flooding. Floods in India, China and Afghanistan caused the greatest number of fatalities, highlighting the high level of vulnerability of Asia, especially to floods. Notable events during the period included:

- Floods, India:** During the monsoon season between June and September, India faced deadly floods. The heavy rain and flash floods resulted in about 1 300 casualties and losses of US\$ 3.1 billion due to damages to crops and properties. However, following a quick response by the authorities, more than 430 000 people were evacuated to safe places<sup>47</sup> (see also [Heavy precipitation and flooding](#)).
- Cyclone Shaheen, Oman:** This cyclone, originating from tropical activity in the Bay of Bengal, tracked westward over India, and made landfall in Oman in October 2021. It was the first storm in 130 years to pass from the east of the Indian subcontinent to the Gulf of Oman and strike the north-eastern coastline. Increased sea-surface temperatures and favourable environmental conditions were the key contributing factors.<sup>48</sup> The intense rainfall, coupled with Oman's varied terrain, resulted in widespread flooding. The Oman Directorate General of Meteorology reports note that six people died in Oman due to the floods, with economic losses of about US\$ 80 million (see also [Tropical cyclones](#)).

- **Sand and dust storms, Saudi Arabia and Kuwait:** Sand and dust storms (SDS) are an emerging concern in the region. In March 2021, SDS affected visibility in northern Saudi Arabia and Kuwait and coincided with the COVID-19 pandemic. As SDS are known to induce respiratory illnesses, the rise in COVID-19 cases was attributed to the storms, with cases increasing 34% in Riyadh<sup>49</sup> and 18% in Kuwait.<sup>50</sup> The Islamic Republic of Iran was also impacted by SDS in 2021 (see also [Other extreme events](#)).

## AGRICULTURE AND FOOD SECURITY

Asia is one of the regions with the highest number of people facing severe food insecurity. According to the *2022 Global Report on Food Crises*, in 2021 three out of the top ten countries with the highest number of people in crisis or worse were in Asia.<sup>51</sup> Climate change-induced extreme weather events exacerbate this vulnerability.

In Afghanistan, 47% of the population experienced high levels of acute food insecurity due to prolonged drought and a struggling economy. Reduced rainfall during the wet season and less snowpack development affected water availability for crops in 2021, which limited availability of food in comparison to other years (see also [Precipitation](#)).<sup>52</sup>

Balochistan, Pakistan, is also an arid zone with a high dependency on rainfall. Between April and November 2021, pre- and post-winter rainfall deficits in this region led to a drought-like state<sup>53</sup> (see also [Droughts](#)). Simultaneously, high food and fuel prices, livestock diseases, and impacts of the COVID-19 pandemic led to a deterioration in food security.<sup>54</sup> Between March and June 2021, approximately 571 000 people were estimated to be at the food insecurity crisis stage and around 185 000 people at the emergency stage. In total, almost 1.18 million people were affected by the drought.<sup>55</sup>

In Nepal, during October, there was an unexpected downpour of rainfall which caused significant loss of agricultural products, lives and property. This rainfall occurred during the end of the harvest season and was estimated to have impacted up to 80% of the harvest<sup>56</sup> (see also [Heavy precipitation and flooding](#)).

## IMPACT ON THE ECONOMY

Comparing the economic loss from disasters in 2021 to the average over the past 20 years shows that damage is on the rise for most types of disasters (Figure 19). More specifically, economic damage from drought has increased by 63%, economic damage from flood has increased by 23% and from landslides by 147% compared to the 2001–2020 average. In 2021, flooding caused the highest economic losses in China (US\$ 18.4 billion), followed by India (US\$ 3.2 billion) and Thailand (US\$ 0.6 billion). Storms also caused significant economic damage, especially in India (US\$ 4.4 billion), China (US\$ 3.0 billion) and Japan (US\$ 2 billion). Extreme heat events are impacting countries around the world through heat stress. Assuming a global temperature increase of 1.5 °C by the end of the twenty-first century, the International Labour Organization (ILO)<sup>57</sup> estimates that by 2030, 2.2% of total working hours will be lost due to heat stress. Given the region's role as an economic hub for manufacturing, the impact of extreme heat events propelled by climate change will be highly disruptive to the economies in the region, with global implications.

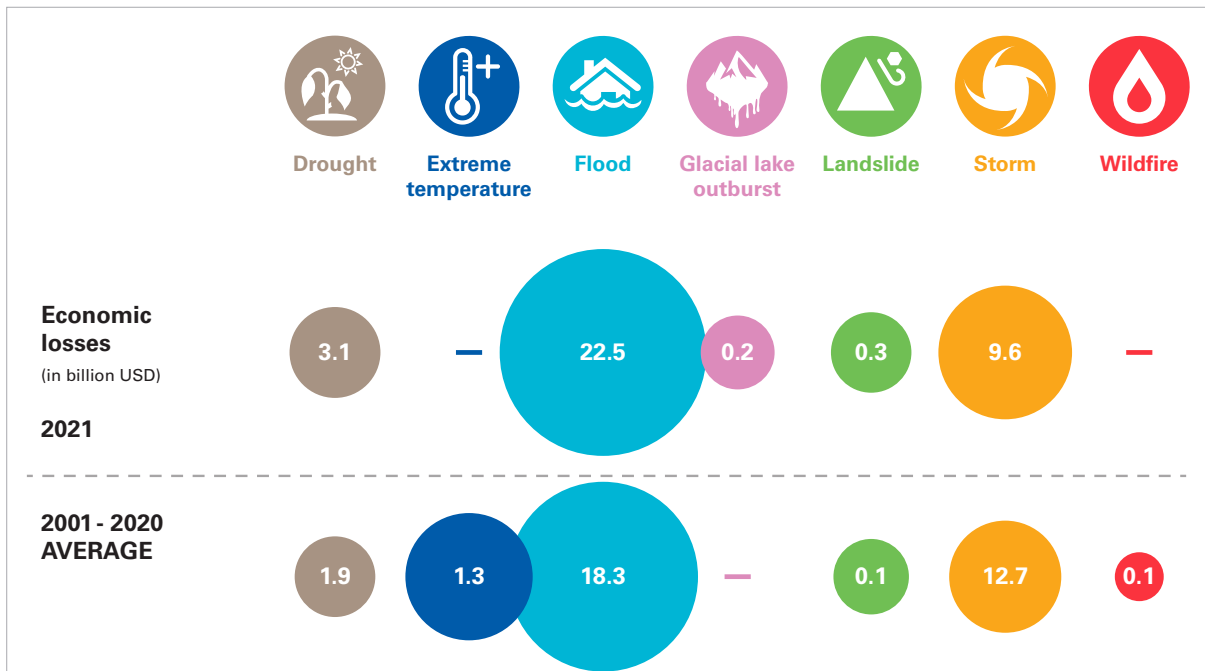


**Figure 19.** Economic losses in Asia in 2021 from disasters, compared to the 20-year average (2001–2020).

Source: ESCAP calculations based on EM-DAT, accessed on 30 April 2022.

Note: The economic damages of some disaster occurrences are not presented in the diagram due to data unavailability

A series of heavy floods caused by excessive rainfall impacted Henan Province and the Inner Mongolia Autonomous regions of China. As a result, about 350 people were killed and many more were recorded as missing. The heavy floods caused over US\$ 16.5 billion in total damage and affected over 14.5 million people. Additionally, 30 600 houses collapsed, and numerous other infrastructures were also impacted by floodwaters.<sup>58</sup> Over 876 000 hectares of farming land was affected due to events linked to the torrential rain<sup>59</sup> (see also [Heavy precipitation and flooding](#)).

From late July to early August 2021, torrential rains and widespread flooding affected Yemen, damaging infrastructure and destroying homes and shelters. Some major infrastructure damage included damage to a bridge linking Lahj Governorate with Ta’iz City, failure of two dams and suspension of operations at several hospital units in Sana’a City.<sup>60</sup> Damage to private property and other structures was reported in one third of Yemen’s districts and across 18 governorates.<sup>61</sup> Furthermore, primary and secondary roads, which were already overdue for maintenance, were damaged, further disrupting access to essential goods and services for citizens.<sup>62</sup>

On 7 January 2021, Hokkaido and central and northern Honshu in Japan experienced severe weather, including large snowfalls, extremely low temperatures and high winds. Preliminary government reports noted 410 disaster-related calamities, while economic losses to agriculture, forestry and fisheries amounted to nearly 12 billion Japanese yen.<sup>63</sup>

# Enhancing climate resilience and adaptation policies

## CLIMATE POLICY AND ACTION

The Paris Agreement, adopted in 2015,<sup>64</sup> identifies adaptation as a global challenge. It establishes the global goal on adaptation, which includes enhancing adaptive capacity, strengthening resilience and reducing vulnerability to climate change. Seven years after its adoption, the Sixth Assessment Report of the IPCC<sup>65</sup> notes that adaptation planning and implementation continues to grow, with at least 170 countries having included adaptation in their policies and planning processes, with decision support tools and climate services in place.

As of June 2022, 194 Parties, of which 31 are from Asia, have submitted a Nationally Determined Contribution (NDC). Mitigation of climate change has been prioritized by all Parties in this region as reflected in their NDCs. These highlight energy, waste, agriculture and land use/land-use change/forestry (LULUCF) as top priority areas for reducing greenhouse gas (GHG) emissions. In terms of GHG emission reduction commitments, some Parties in the region have strengthened their targets, although still more needs to be done in order to keep the region and the world within the 1.5 °C global temperature rise. In addition, 90% of Asian Parties have prioritized adaptation in their NDCs, with the majority highlighting the following as their top priority areas for adaptation: water; agriculture and food security; ecosystem and biodiversity; and health (Figure 20). Over 80% of Parties in the region have prioritized in their NDCs climate services-related activities<sup>66</sup> in areas shown in Figure 20, with the majority being the least developed countries (LDCs) and small island development States (SIDS).

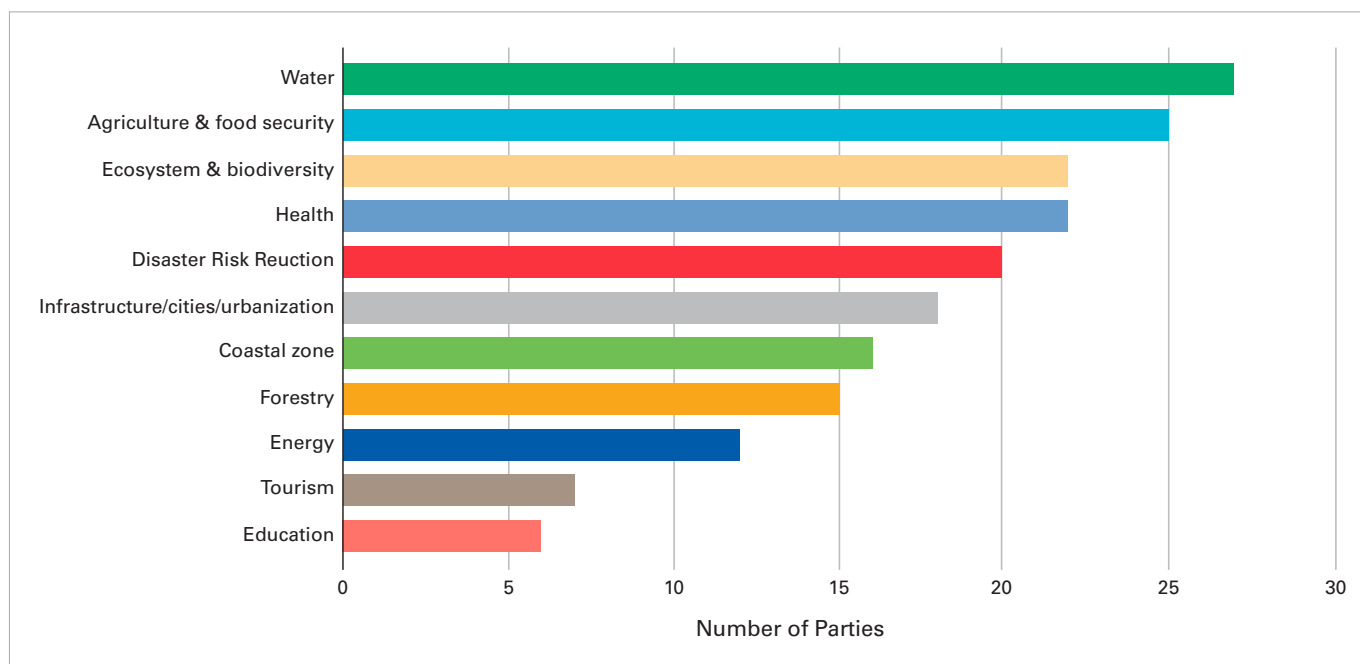


**Figure 20.** Priority areas for adaptation for the Asia region. *Source:* WMO analysis of the NDCs of 31 Parties in Asia from 2016 to March 2022, updated in June 2022

However, there are still adaptation gaps between the current levels of adaptation and the levels needed to respond to climate risks and impacts. The *Asia-Pacific Disaster Reports for 2021 and 2022*<sup>67</sup> estimate the annual adaptation cost for climate and biological hazards<sup>68</sup> in each country under the RCP 8.5 climate change scenario (that is, a high greenhouse gas emission future without effective climate change mitigation policies and used in the assessment in the IPCC Fifth Assessment Report<sup>69</sup>). In Asia, the highest adaptation cost is estimated for China at US\$ 188.8 billion, followed by India at US\$ 46.3 billion, and Japan at US\$ 26.5 billion. As a percentage of the country's gross domestic product (GDP), the highest cost is estimated for Nepal at 1.9% of GDP, followed by Cambodia at 1.8%, and India at 1.7%.

A key driver of policy action is the target to achieve the global 2030 Agenda for Sustainable Development, pillared on the 17 Sustainable Development Goals (SDGs). The United Nations Economic and Social Commission for Asia and the Pacific (ESCAP) *Asia and the Pacific SDG Progress Report 2022*<sup>70</sup> shows that none of the goals have been sufficiently achieved. In fact, Goal 13 on Climate Action continues to show a reverse trend. There is insufficient progress on achieving targets such as 13.1.1 on the number of deaths, missing persons and directly affected persons attributed to disasters, and 13.1.2 on adoption and implementation of national disaster risk reduction strategies.

## MEMBERS' CAPACITIES: CLIMATE SERVICES AND EARLY WARNING

In Asia, from 1970–2019, about 3 500 reported disasters led to nearly 1 000 000 deaths, and economic losses of US\$ 1.2 trillion. Most of these disasters were associated with floods (45%) and storms (36%). Storms had the highest impacts on life, contributing to 72% of the lives lost, while floods led to the greatest economic losses (57%) (Figure 21). Specifically, from 1970–2019, more than 1 500 flood-related disasters led to nearly 230 000 deaths, and economic losses of US\$ 683 billion in Asia. These numbers are quite high compared to other regions.<sup>71</sup>

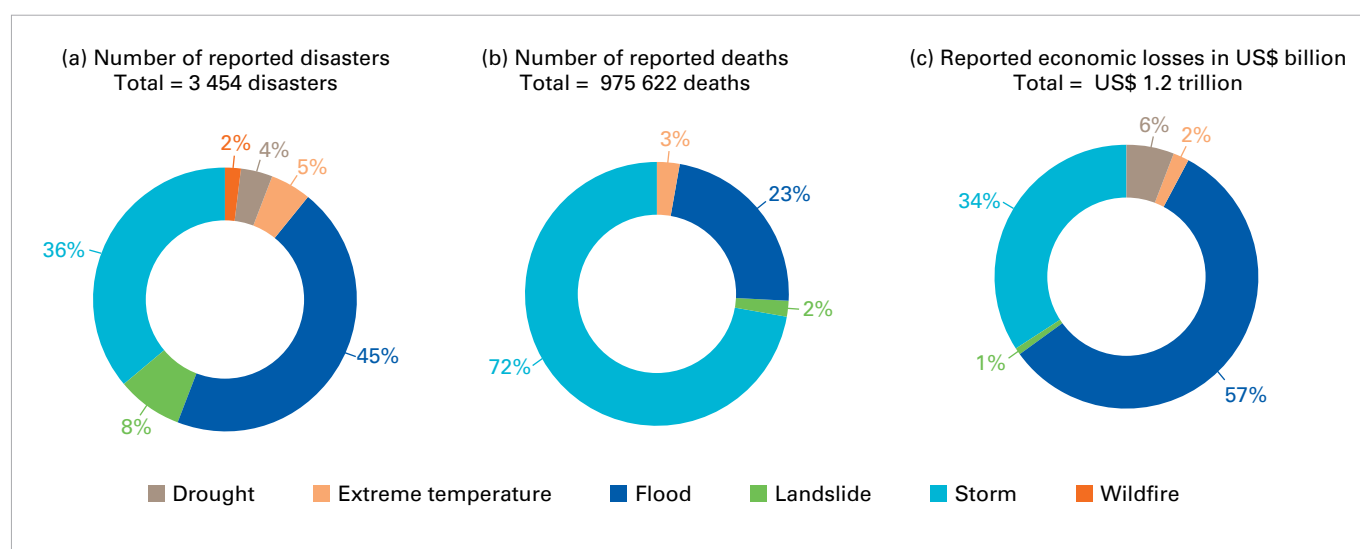


**Figure 21.** Overview of weather-, water- and climate-related disasters, deaths and economic losses reported in Asia (1970–2019).  
Source: *2021 State of the Climate Service: Water* (WMO-No. 1278).

In this context, and building on five adaptation priorities highlighted by the Global Commission on Adaptation<sup>72</sup> with high investment cost-benefits, top adaptation priorities informed by the risk landscape in Asia can be identified. In Asia, the key adaptation priorities are strengthening the early warning systems and building new, resilient infrastructure, followed by making water resources management more resilient, improving dryland agriculture crop production and implementing nature-based solutions. Investing in these policy actions will catalyse progress in achieving multiple SDGs as well as yield cross-sectoral benefits, aligned with the NDCs and National Adaptation Plan (NAP) commitments of countries in Asia.

In 2021, floods and storms caused the highest fatalities as well as economic losses in Asia (Figure 18). Strengthening early warning systems can play a pivotal role in taking anticipatory action, enhancing preparedness and reducing the impact of these hazards, as indicated in Figure 22. Early warning systems not only protect lives and livelihoods, but also help protect development gains in the long term.<sup>73</sup>

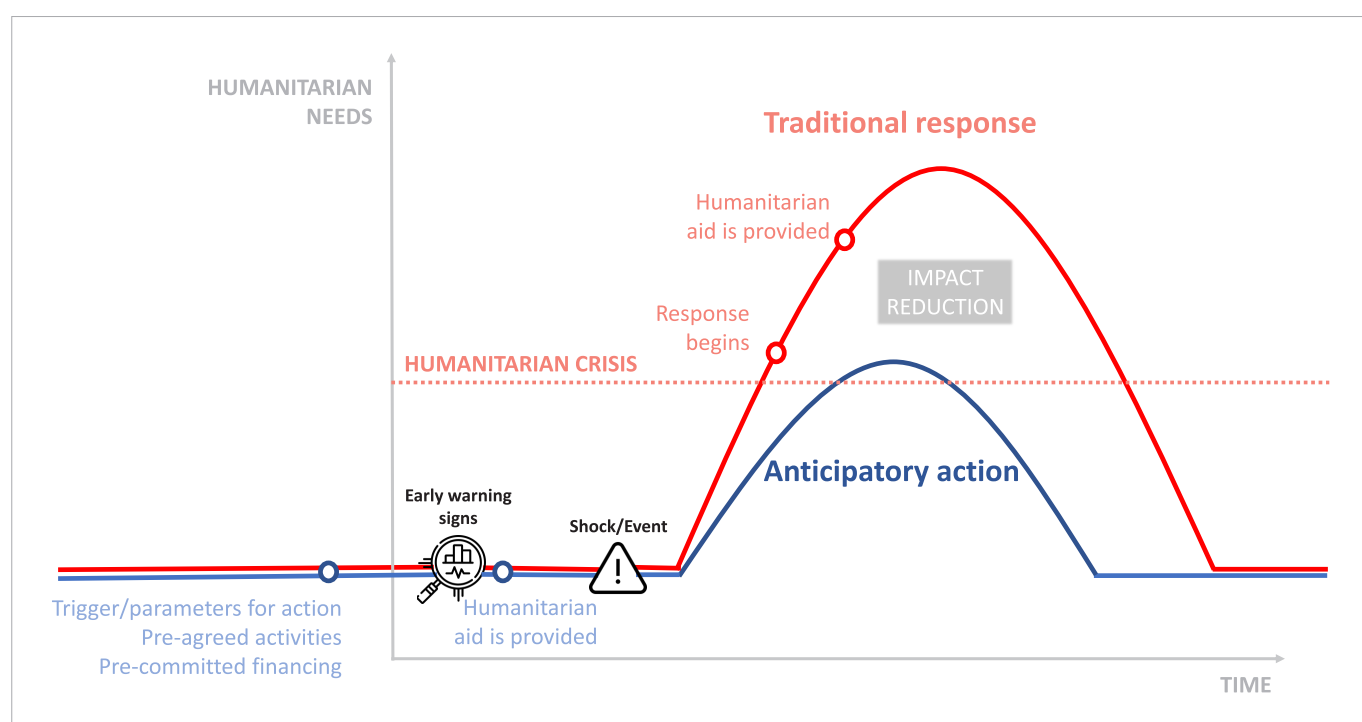


**Figure 22.** Tackling the extent of humanitarian crises by anticipatory action.  
 Source: The Economic and Social Commission for Asia and the Pacific (ESCAP).

WMO data from 24 countries for which data are available, show that most Members (50%) in the region provide climate services at an average level, while 17% of the Members provide climate services at a basic level (as of 16 June 2022).

Two Members in this region report having inadequate end-to-end riverine flood forecasting services, and nine Members are providing those services at a Full/Advanced capacity level. Ten Members indicate having inadequate end-to-end drought forecasting systems, and four are providing drought warning services at a Full/Advanced capacity level. Additionally, only five Members indicate providing flash floods warnings at a Full/Advanced capacity level, despite flash floods being among the most common weather, water and climate disasters in the region (Figure 23).

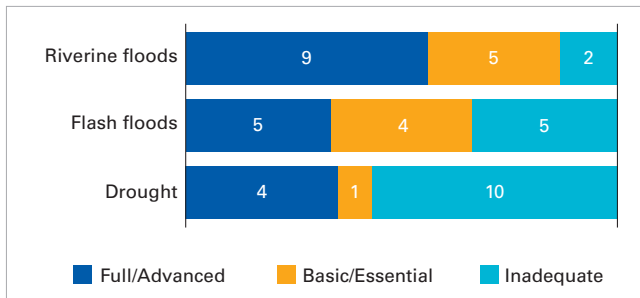


**Figure 23.** Number of WMO Members in Asia with early warnings available to the population at risk, by hazard type, based on data provided by WMO Members. Member capacities are categorized as Inadequate (0–33%), Basic/Essential (34–66%) and Full/Advanced (67–100%) according to the estimated percentage of the population at risk that receive early warnings. Note: For each hazard, the category “Inadequate” includes Members (providing data) reporting that no end-to-end early warning system (EWS) for the hazard is in place, as well as those whose end-to-end EWSs do not reach more than 33% of the at-risk population.<sup>74</sup>

Substantially increasing availability and access to early warning systems and disaster risk reduction information is a key target of the Sendai Framework for Disaster Risk Reduction 2015–2030.<sup>75</sup> As shown in Figure 23, there is still room for improvement for deployment of fully operational early warning systems for riverine floods, flash floods and drought. It should be noted that the data were only obtained from a very limited number of WMO Members, and there is a substantial need for improved data from all Members in the region, in order to obtain a clearer picture of the gaps and needs moving forward. However, there is also a clear need to prioritize the development of multi-hazard early warning systems and climate forecasts, not only for tackling natural hazards and achieving SDG 13 (Climate Action), but also for accelerating progress on multiple associated SDGs including 1 (No Poverty), 2 (Zero Hunger), 3 (Good Health and Well-being), 9 (Industry, Innovation and Infrastructure) and 11 (Sustainable Cities and Communities). With this objective in mind, the United Nations ESCAP Asia-Pacific Risk and Resilience Portal<sup>76</sup> is designed to support the monitoring and implementation of climate and disaster-related SDGs. It aims to strengthen the capacity of Members in Asia and the Pacific to identify multi-hazard risk hotspots, estimate economic losses due to cascading hazards in the present and future climate change scenarios at the country, subregional and regional levels, and invest in key resilience measures for adaptation.



# Data sets

## TEMPERATURE

Six data sets (cited below) were used in the calculation of regional temperature.

Regional mean temperature anomalies were calculated relative to 1961–1990 and 1981–2010 baselines using the following steps:

1. Read the gridded data set;
2. Regrid the data to 1° latitude × 1° longitude resolution. If the gridded data are higher resolution, then take a mean of grid boxes within each 1° × 1° grid box. If the gridded data are lower resolution, then copy the low-resolution grid box value into each 1° × 1° grid box that falls inside the low-resolution grid box;
3. For each month, calculate the regional area average using only those 1° × 1° grid boxes whose centres fall within the region;
4. For each year, take the mean of the monthly area averages to obtain an annual area average;
5. Calculate the mean of the annual area averages over the periods 1961–1990 and 1981–2010;
6. Subtract the 30-year period average from each year.

Note that the range and mean of anomalies relative to the two different baselines are based on different sets of data, as anomalies relative to 1961–1990 cannot be computed for ERA5 which starts in 1979.

The following six data sets were used:

Berkeley Earth – Rohde, R. A.; Hausfather, Z. The Berkeley Earth Land/Ocean Temperature Record. *Earth System Science Data* **2020**, 12 (4), 3469–3479. <https://doi.org/10.5194/essd-12-3469-2020>.

ERA5 – Hersbach, H.; Bell, B.; Berrisford, P. et al. The ERA5 Global Reanalysis. *Quarterly Journal of the Royal Meteorological Society* **2020**, 146 (730), 1999–2049. <https://doi.org/10.1002/qj.3803>.

JRA-55 – Kobayashi, S.; Ota, Y.; Harada, Y. et al. The JRA-55 Reanalysis: General Specifications and Basic Characteristics. *Journal of the Meteorological Society of Japan. Ser. II* **2015**, 93 (1), 5–48. [https://www.jstage.jst.go.jp/article/jmsj/93/1/93\\_2015-001/\\_article](https://www.jstage.jst.go.jp/article/jmsj/93/1/93_2015-001/_article).

GISTEMP v4 – GISTEMP Team, 2022: GISS Surface Temperature Analysis (GISTEMP), version 4. NASA Goddard Institute for Space Studies, <https://data.giss.nasa.gov/gistemp/>. Lenssen, N.; Schmidt, G.; Hansen, J. et al. Improvements in the GISTEMP Uncertainty Model. *Journal of Geophysical Research: Atmospheres* **2019**, 124 (12), 6307–6326. <https://doi.org/10.1029/2018JD029522>.

HadCRUT.5.0.1.0 – Morice, C. P.; Kennedy, J. J.; Rayner, N. A. et al. An Updated Assessment of Near-Surface Temperature Change From 1850: The HadCRUT5 Data Set. *Journal of Geophysical Research: Atmospheres* **2021**, 126 (3), e2019JD032361. <https://doi.org/10.1029/2019JD032361>. HadCRUT.5.0.1.0 data were obtained from <http://www.metoffice.gov.uk/hadobs/hadcrut5> and are © British Crown Copyright, Met Office 2021, provided under an Open Government License, <http://www.nationalarchives.gov.uk/doc/open-government-licence/version/3/>.

NOAAGlobalTemp v5 – Zhang, H.-M.; Huang, B.; Lawrimore, J. et al. NOAA Global Surface Temperature Dataset (NOAAGlobalTemp), Version 5.0. *NOAA National Centers for Environmental Information*. doi:10.7289/V5FN144H. Huang, B.; Menne, M. J.; Boyer, T. et al. Uncertainty Estimates for Sea Surface Temperature and Land Surface Air Temperature in NOAAGlobalTemp Version 5. *Journal of Climate* **2020**, 33 (4), 1351–1379. <https://journals.ametsoc.org/view/journals/clim/33/4/jcli-d-19-0395.1.xml>.

## PRECIPITATION

Regional time series analyses of the area-mean annual precipitation totals are from the Global Precipitation Climatology Centre (GPCC). Regional precipitation anomalies are expressed relative to the 1981–2010 average. Schneider, U.; Becker, A.; Finger, P. et al. *GPCC Monitoring Product: Near Real-Time Monthly Land-Surface Precipitation from Rain-Gauges Based on SYNOP and CLIMAT Data*; Global Precipitation Climatology Centre (GPCC), 2020. [https://opendata.dwd.de/climate\\_environment/GPCC/html/gpcc\\_monitoring\\_v2020\\_doi\\_download.html](https://opendata.dwd.de/climate_environment/GPCC/html/gpcc_monitoring_v2020_doi_download.html).

## SEA ICE

In the present report, the estimation of sea-ice extent is based on an analysis of blended Arctic ice charts from the Arctic and Antarctic Research Institute (Russian Federation), the Canadian Ice Service (Canada) and the National Ice Center (United States of America), using passive microwave estimates (SMMR, SSM/I and SSMIS) from the National Snow and Ice Data Center.

## SEA LEVEL

Regional sea-level trends are based on gridded C3S altimetry data, averaged from the 50 km offshore to the coast, by the Laboratory of Space Geophysical and Oceanographic Studies (LEGOS).

## EM-DAT DATA

EM-DAT data were used for historical climate impact calculations: [www.emdat.be](http://www.emdat.be). EM-DAT is a global database on natural and technological disasters, containing essential core data on the occurrence and effects of more than 21 000 disasters in the world, from 1900 to the present. EM-DAT is maintained by the Centre for Research on the Epidemiology of Disasters (CRED) at the School of Public Health of the Université catholique de Louvain located in Brussels, Belgium.

The indicators used for mortality, number of people affected and economic damage were total deaths, number affected and total damages ('000 US\$) respectively.

## CLIMATE SERVICES

WMO Analysis of NDCs;

Checklist for Climate Services Implementation (Members' climate services capacity, based on responses to this Checklist, can be viewed [here](#));

[WMO Hydrology Survey, 2020](#);

[2020 State of Climate Services: Risk Information and Early Warning Systems](#) (WMO-No. 1252);

[2021 State of Climate Services: Water](#) (WMO-No. 1278).

# List of contributors

## CONTRIBUTING EXPERTS (IN ALPHABETICAL ORDER BY SURNAME):

Sreejith Op (Lead, India), Sanjay Srivastava (Lead, ESCAP), Peiqun Zhang (Lead, China), Shashwat Avi (ESCAP), Omar Baddour (WMO), Antonio Bombelli (WMO), Anny Cazenave (LEGOS), Carol Chouchani Cherfane (ESCWA), Maria Bernadet Karina Dewi (ESCAP), Sarah Diouf (WMO), Sapna Dubey (ESCAP), Atsushi Goto (WMO), Veronica Grasso (WMO), Peer Hechler (WMO), Phuc Lam Hoang (Viet Nam), Soomi Hong (ESCAP), Catherine Jones (FAO), Hideli Kanamaru (FAO), Valentina Khan (Russian Federation), Jinwon Kim (Republic of Korea), Lijuan Ma (China), Cristina Martinez (ILO), Belén Martín Míguez (WMO), Atsushi Minami (Japan), Nakiete Msemo (WMO), Noboru Nemoto (Japan), Tim Oakley (WMO), HangThiThanh Pham (FAO), Claire Ransom (WMO), Anthony Rea (WMO), Eric Roeder (ILO), Tarek Sadek (ESCWA), Madhurima Sarkar-Swaigood (ESCAP), Karina Von Schuckmann (Mercator Ocean), Jose Alvaro Silva (WMO), Kiyotoshi Takahashi (Japan), Caterina Tassone (WMO), Marlene Ann Tomaszkiwicz (ESCWA), Muhibuddin Usamah (WMO), Ahad Vazifeh (Islamic Republic of Iran), Shunya Wakamatsu (Japan), Pengling Wang (China), Markus Ziese (Germany)

## EXPERT TEAM ON CLIMATE MONITORING AND ASSESSMENT (REVIEWERS)

John Kennedy (Lead, United Kingdom), Jessica Blunden (Co-Lead, United States of America), Randall S. Cerveny (United States of America), Ladislaus Benedict Chang'a (United Republic of Tanzania), Liudmila Kolomeets (Russian Federation), Renata Libonati (Brazil), Awatif Ebrahim Mostafa (Egypt), Serhat Sensoy (Türkiye), Ardhasena Sopaheluwakan (Indonesia), Jose Luis Stella (Argentina), Freja Vamborg (European Centre for Medium-Range Weather Forecasts, ECMWF), Zhiwei Zhu (China)

## CONTRIBUTING ORGANIZATIONS

Food and Agriculture Organization of the United Nations (FAO), International Labour Organization (ILO), Laboratory of Space Geophysical and Oceanographic Studies (LEGOS), Mercator Ocean International, United Nations Economic and Social Commission for Asia and the Pacific (ESCAP), United Nations Economic and Social Commission for Western Asia (ESCWA), World Food Programme (WFP), World Meteorological Organization (WMO)

## CONTRIBUTING WMO MEMBERS (IN ALPHABETICAL ORDER)

Bahrain; China; Hong Kong, China; India; Islamic Republic of Iran; Japan; Macao, China; Oman; Pakistan; Republic of Korea; Russian Federation; Saudi Arabia; Thailand; United Arab Emirates; Uzbekistan; Viet Nam

## Endnotes

- 1 World Meteorological Organization (WMO). *WMO Greenhouse Gas Bulletin, No. 17: The State of Greenhouse Gases in the Atmosphere Based on Global Observations through 2020*; WMO: Geneva, 2021.
- 2 World Meteorological Organization (WMO). *State of the Global Climate 2021* (WMO-No. 1290). Geneva, 2022.
- 3 Intergovernmental Panel on Climate Change (IPCC). *Climate Change 2021: The Physical Science Basis. Contribution of Working Group I to the Sixth Assessment Report of the Intergovernmental Panel on Climate Change*; Masson-Delmotte, V.; Zhai, P.; Pirani, A. et al. Eds. Cambridge University Press, Cambridge, United Kingdom and New York, USA, 2021. <https://www.ipcc.ch/report/sixth-assessment-report-working-group-i/>.
- 4 WMO Regional Association II (Asia)
- 5 China Meteorological Administration (CMA) Beijing Climate Centre. *Blue Book on Climate Change in China 2022*. Science Press: Beijing, 2022.
- 6 Arctic Regional Climate Centre Network (ArcRCC-Network). *Arctic Climate Forum Consensus Statement: 2021 Arctic Summer Seasonal Climate Outlook (Along with a Summary of 2020–2021 Arctic Winter Season)*; The 7th Session of the Arctic Climate Forum (ACF), 26–27 May 2021. [https://arctic-rcc.org/sites/arctic-rcc.org/files/documents/acf-spring-2021/ACF-7\\_Consensus\\_Statement\\_final.pdf](https://arctic-rcc.org/sites/arctic-rcc.org/files/documents/acf-spring-2021/ACF-7_Consensus_Statement_final.pdf).
- 7 The statement was based on data from passive microwave sounding SSMR-SSM/I-SSMIS by the National Snow and Ice Data Center (NSIDC) and calculated at the World Sea-ice Data Center at the Arctic and Antarctic Research Institute.
- 8 Arctic Regional Climate Centre Network ArcRCC-Network. *Arctic Climate Forum Consensus Statement: 2021–2022 Arctic Winter Seasonal Climate Outlook (Along with a Summary of 2021 Arctic Summer Season)*. The 8th session of the Arctic Climate Forum (ACF), 27–28 October 2021. [https://arctic-rcc.org/sites/arctic-rcc.org/files/documents/acf-fall-2021/ACF-8\\_Consensus\\_Statement\\_Final.pdf](https://arctic-rcc.org/sites/arctic-rcc.org/files/documents/acf-fall-2021/ACF-8_Consensus_Statement_Final.pdf).
- 9 United Nations Environment Programme (UNEP). *A Scientific Assessment of the Third Pole Environment*; UNEP: Nairobi, 2022. <https://wedocs.unep.org/20.500.11822/39757>.
- 10 Yao, T.; Xue, Y.; Chen, D. et al. Recent Third Pole's Rapid Warming Accompanies Cryospheric Melt and Water Cycle Intensification and Interactions between Monsoon and Environment: Multidisciplinary Approach with Observations, Modeling, and Analysis. *Bulletin of the American Meteorological Society* **2019**, *100* (3), 423–444. <https://doi.org/10.1175/BAMS-D-17-0057.1>.
- 11 World Glacier Monitoring Service (WGMS). *Global Glacier Change Bulletin No. 4 (2018–2019)*; Zemp, M; Nussbaumer, S. U.; Gärtner-Roer, I. et al. Eds.; WGMS: Zurich, 2021.
- 12 Yao, T.; Thompson, L.; Yang, W. et al. Different Glacier Status with Atmospheric Circulations in Tibetan Plateau and Surroundings. *Nature Climate Change* **2012**, *2*, 663–667. <http://doi.org/10.1038/nclimate1580>.
- 13 Anisimov, O. A.; Lavrov, S. A.; Zhirkov, A. F. et al. Permafrost Data Assimilation and Reanalysis: Computational Setup and Model Validation for North-European Russia and East Siberia. *Russian Meteorology and Hydrology* **2020**, *45*, 269–275. <https://doi.org/10.3103/S106837392004007X>. Anisimov, O. A. Potential Feedback of Thawing Permafrost to the Global Climate System through Methane Emission. *Environmental Research Letters* **2007**, *2* (4), 91–98. <http://dx.doi.org/10.1088/1748-9326/2/4/045016>.
- 14 Russian Federal Service for Hydrometeorology and Environmental Monitoring (RosHydroMet). *A Report on Climate Features on the Territory of the Russian Federation in 2021* (in Russian); Moscow, 2022. <https://www.meteorf.gov.ru/images/news/20220324/4/Doklad.pdf>. The monitoring results are based on the daily ground temperature observations at standardized depths up to 3.2 m (320 cm) at 146 weather stations in the permafrost regions of the Russian Federation.
- 15 Defined as the fraction of the total incident solar radiation reflected by the Earth back to space
- 16 Russian Federal Service for Hydrometeorology and Environmental Monitoring (RosHydroMet). *A Report on Climate Features on the Territory of the Russian Federation in 2021* (in Russian); Moscow, 2022. <https://www.meteorf.gov.ru/images/news/20220324/4/Doklad.pdf>.
- 17 Gulev, S. K.; Thorne, P. W.; Ahn, J. et al. Changing State of the Climate System. In *Climate Change 2021: The Physical Science Basis. Contribution of Working Group I to the Sixth Assessment Report of the Intergovernmental Panel on Climate Change*; Masson-Delmotte, V.; Zhai, P.; Pirani, A. et al., Eds. Cambridge University Press: Cambridge, United Kingdom and New York, USA, 2021. <https://www.ipcc.ch/report/ar6/wg1/>.
- 18 Copernicus Marine Service (CMEMS). *Global Mean Sea Surface Temperature, Ocean Monitoring Indicator Framework*, 2021. <https://marine.copernicus.eu/access-data/ocean-monitoring-indicators/global-ocean-anomaly-time-series-sea-surface-temperature>.

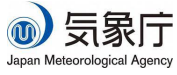
- 19 Schlichtholz, P. Subsurface Ocean Flywheel of Coupled Climate Variability in the Barents Sea Hotspot of Global Warming. *Scientific Reports* **2019**, *9*. <https://doi.org/10.1038/s41598-019-49965-6>.
- 20 Dai, A.; Luo, D.; Song, M. et al. Arctic Amplification is Caused by Sea-ice Loss under Increasing CO<sub>2</sub>. *Nature Communications* **2019**, *10*. <https://doi.org/10.1038/s41467-018-07954-9>.
- 21 Aaboe, S.; Lind, S.; Hendricks, S. et al. Section 4.1. Sea-ice and Ocean Conditions Surprisingly Normal in the Svalbard-Barents Sea Region After Large Sea-ice Inflows in 2019. In The Copernicus Marine Service Ocean State Report, Issue 5, von Schuckmann, K.; Le Traon, P.-Y.; Smith, N. Eds.; *Journal of Operational Oceanography* **2021**, *14*. <https://doi.org/10.1080/1755876X.2021.1946240>.
- 22 Kumar, A.; Yadav, J.; Mohan, R. Spatio-temporal Change and Variability of Barents-Kara Sea Ice, in the Arctic: Ocean and Atmospheric Implications. *Science of The Total Environment* **2021**, *753*. <https://doi.org/https://doi.org/10.1016/j.scitotenv.2020.142046>.
- 23 Intergovernmental Panel on Climate Change (IPCC). *IPCC Special Report on the Ocean and Cryosphere in a Changing Climate*; Pörtner, H.-O.; Roberts, D.C.; Masson-Delmotte, V. et al. Eds. Cambridge University Press: Cambridge, UK and New York, USA, 2019. <https://www.ipcc.ch/srocc/>.
- 24 von Schuckmann, K.; Cheng, L.; Palmer, M. D. et al. Heat Stored in the Earth System: Where Does the Energy Go? *Earth System Science Data* **2020**, *12* (3), 2013–2041. <https://doi.org/10.5194/essd-12-2013-2020>.
- 25 Oppenheimer, M.; Glavovic, B. C.; Hinkel, J. et al. Sea Level Rise and Implications for Low-Lying Islands, Coasts and Communities. In: *IPCC Special Report on the Ocean and Cryosphere in a Changing Climate*; Pörtner, H.-O.; Roberts, D.C.; Masson-Delmotte, V. et al. Eds. Cambridge University Press: Cambridge, UK and New York, USA, 2019. <https://www.ipcc.ch/srocc/>.
- 26 Intergovernmental Panel on Climate Change (IPCC). *Global warming of 1.5 °C. An IPCC Special Report on the Impacts of Global Warming of 1.5 °C Above Pre-industrial Levels and Related Global Greenhouse Gas Emission Pathways, in the Context of Strengthening the Global Response to the Threat of Climate Change, Sustainable Development, and Efforts to Eradicate Poverty*; Masson-Delmotte, V.; Zhai, P.; Pörtner, H. O. et al. Eds. Cambridge University Press: Cambridge, UK and New York, USA, 2018. <https://www.ipcc.ch/sr15/>.
- 27 Li, G.; Cheng, L.; Zhu, J. et al. Increasing Ocean Stratification over the Past Half-century. *Nature Climate Change* **2020**, *10*, 1116–1123 . <https://doi.org/10.1038/s41558-020-00918-2>.
- 28 Intergovernmental Panel on Climate Change (IPCC). *IPCC Special Report on the Ocean and Cryosphere in a Changing Climate*; Pörtner, H.-O.; Roberts, D.C.; Masson-Delmotte, V. et al. Eds. Cambridge University Press: Cambridge, UK and New York, USA, 2019. <https://www.ipcc.ch/srocc/>.
- 29 Hamlington, B. D.; Frederikse, T.; Nerem, R. S. et al. Investigating the Acceleration of Regional Sea Level Rise During the Satellite Altimeter Era. *Geophysical Research Letters* **2020**, *47* (5). <http://dx.doi.org/10.1029/2019GL086528>.
- 30 Cazenave, A.; Moreira, L. Contemporary Sea-level Changes from Global to Local Scales: A Review. *Proceedings of the Royal Society A* **2022**. *478* (2261). <https://doi.org/10.1098/rspa.2022.0049>.
- 31 Tokyo Climate Center. *Impacts of El Niño/La Niña and Indian Ocean Dipole Events on the Global Climate*, <http://ds.data.jma.go.jp/tcc/tcc/products/climate/ENSO/index.htm>.
- 32 [https://ds.data.jma.go.jp/tcc/tcc/news/press\\_20220201.pdf](https://ds.data.jma.go.jp/tcc/tcc/news/press_20220201.pdf)
- 33 Meiyu/Baiu/Changma is the major rainy season from central China to Japan and Korea, brought by a zonally elongated rainband caused by the East Asia summer monsoon from June to July. It is called Meiyu in China, Baiu in Japan, and Changma in Korea.
- 34 Pai D. S.; Bandgar, A.; Devi, S. et al. Normal Dates of Onset/Progress and Withdrawal of Southwest Monsoon over India. *MAUSAM* **2020**, *71* (4), 553–570. <https://doi.org/10.54302/mausam.v71i4.33>.
- 35 Ralph, F. M.; Neiman, P. J.; Wick, G. A. Satellite and CALJET Aircraft Observations of Atmospheric Rivers over the Eastern North Pacific Ocean during the Winter of 1997/98. *Monthly Weather Review* **2004**, *132* (7), 1721–1745. [https://doi.org/10.1175/1520-0493\(2004\)132%3C1721:SACAO%3E2.0.CO;2](https://doi.org/10.1175/1520-0493(2004)132%3C1721:SACAO%3E2.0.CO;2).
- 36 Neiman, P. J.; Ralph, F. M.; Wick, G. A. et al. Meteorological Characteristics and Overland Precipitation Impacts of Atmospheric Rivers Affecting the West Coast of North America Based on Eight Years of SSM/I Satellite Observations. *Journal of Hydrometeorology* **2008**, *9* (1), 22–47. <https://doi.org/10.1175/2007JHM855.1>.
- 37 Dettinger, M. D.; Ralph, F. M.; Das, T. et al. Atmospheric Rivers, Floods and the Water Resources of California. *Water* **2011**, *3* (2), 445–478. <https://doi.org/10.3390/w3020445>.
- 38 Lavers, D. A.; Villarini, G. Atmospheric Rivers and Flooding over the Central United States, *Journal of Climate* **2013**, *26* (20), 7829–7836. <https://doi.org/10.1175/JCLI-D-13-00212.1>.
- 39 Paltan, H.; Waliser, D.; Lim, W. H. et al. Global Floods and Water Availability Driven by Atmospheric Rivers. *Geophysical Research Letters* **2017**, *44* (20), 10387–10395. <https://doi.org/10.1002/2017GL074882>.

- 40 Kim, J.; Guan, B.; Waliser, D. E. et al. Winter Precipitation Characteristics in Western US Related to Atmospheric River Landfalls: Observations and Model Evaluations. *Climate Dynamics* **2018**, *50*, 231–248. <https://link.springer.com/article/10.1007/s00382-017-3601-5>.
- 41 Park, C.; Son, S.-W.; Kim, H. Distinct Features of Atmospheric Rivers in the Early Versus Late East Asian Summer Monsoon and their Impacts on Monsoon Rainfall. *Journal of Geophysical Research Atmospheres* **2021**, *126* (7). <https://doi.org/10.1029/2020JD033537>.
- 42 RSMC Tokyo – Typhoon Center, <http://www.jma.go.jp/jma/jma-eng/jma-center/rsmc-hp-pub-eg/climatology.html>
- 43 <https://reliefweb.int/report/pakistan/drought-bulletin-pakistan-june-2021>
- 44 <https://reliefweb.int/disaster/dr-2021-000089-irn>
- 45 <https://reliefweb.int/disaster/dr-2021-000119-irq>
- 46 National contribution, Russian Federation
- 47 Humanitarian Aid International (HAI): *Current situation on Maharashtra Floods and Landslides*; Reliefweb, 03 August 2021. <https://reliefweb.int/report/india/current-situation-maharashtra-floods-and-landslides-date-03-08-2021>.
- 48 Terry, J.; Ruheili, A.; Boldi, R. et al. Cyclone *Shaheen*: The Exceptional Tropical Cyclone of October 2021 in the Gulf of Oman. *Royal Meteorological Society* **2022**, *77* (10), 364–370. <https://doi.org/10.1002/wea.4193>.
- 49 Meo, S. A.; Almutairi, F. J.; Abukhalaf, A. A. et al. Sandstorm and Its Effect on Particulate Matter PM2.5, Carbon Monoxide, Nitrogen Dioxide, Ozone Pollutants and SARS-CoV-2 Cases and Deaths. *Science of the Total Environment* **2021**, *795*. DOI:10.1016/j.scitotenv.2021.148764.
- 50 Meo, S. A.; Almutairi, F. J.; Abukhalaf, A. A. et al. Impact of Sandstorm on Environmental Pollutants PM2.5, Carbon Monoxide, Nitrogen Dioxide, Ozone, and SARS-CoV-2 Morbidity and Mortality in Kuwait. *Journal of King Saud University-Science* **2022**, *34* (5). DOI:10.1016/j.jksus.2022.102109.
- 51 Food and Agriculture Organization of the United Nations (FAO); International Food Policy Research Institute (IFPRI); World Food Programme (WFP). *2022 Global Report on Food Crises*; FAO: Rome, 2022. <https://www.wfp.org/publications/global-report-food-crises-2022>.
- 52 Integrated Food Security Phase Classification (IPC). *Afghanistan: IPC Acute Food Insecurity Analysis, September 2021–March, 2022*. [https://www.ipcinfo.org/fileadmin/user\\_upload/ipcinfo/docs/IPC\\_Afghanistan\\_AcuteFoodInsec\\_2021Oct2022Mar\\_report.pdf](https://www.ipcinfo.org/fileadmin/user_upload/ipcinfo/docs/IPC_Afghanistan_AcuteFoodInsec_2021Oct2022Mar_report.pdf).
- 53 Integrated Food Security Phase Classification (IPC). *Balochistan, Pakistan: IPC Acute Food Insecurity Analysis, March–September, 2021*. [https://www.ipcinfo.org/fileadmin/user\\_upload/ipcinfo/docs/IPC\\_Pakistan\\_Balochistan\\_Acute\\_Food\\_Insecurity\\_2021MarSept\\_Report.pdf](https://www.ipcinfo.org/fileadmin/user_upload/ipcinfo/docs/IPC_Pakistan_Balochistan_Acute_Food_Insecurity_2021MarSept_Report.pdf).
- 54 Integrated Food Security Phase Classification (IPC). *Balochistan, Pakistan: IPC Acute Food Insecurity Analysis, March–September, 2021*. [https://www.ipcinfo.org/fileadmin/user\\_upload/ipcinfo/docs/IPC\\_Pakistan\\_Balochistan\\_Acute\\_Food\\_Insecurity\\_2021MarSept\\_Report.pdf](https://www.ipcinfo.org/fileadmin/user_upload/ipcinfo/docs/IPC_Pakistan_Balochistan_Acute_Food_Insecurity_2021MarSept_Report.pdf).
- 55 Food and Agriculture Organization of the United Nations (FAO); World Food Programme (WFP). *Drought Situation Report: Pakistan, Volume 1, Issue 2*; 31 May 2021. <https://reliefweb.int/report/pakistan/drought-situation-report-pakistan-volume-1-issue-ii-may-31-2021>.
- 56 International Federation of Red Cross and Red Crescent Societies. *Nepal: Monsoon Floods and Landslides – Operation Update Report #1*; 5 November 2021. <https://reliefweb.int/report/nepal/nepal-monsoon-floods-and-landslides-operation-update-1-dref-operation-n-mdrnp011>.
- 57 International Labour Organization (ILO). *Working on a Warmer Planet: The Impact of Heat Stress on Productivity and Decent Work*; ILO: Geneva, 2019. [https://www.ilo.org/global/publications/books/WCMS\\_711919/lang--en/index.htm](https://www.ilo.org/global/publications/books/WCMS_711919/lang--en/index.htm).
- 58 European Commission Directorate-General for European Civil Protection and Humanitarian Aid Operations (ECHO). *China Floods Update (People’s Government of Henan Province, CMA)*; ECHO Daily Flash, 03 August 2021. <https://reliefweb.int/report/china/china-floods-update-peoples-government-henan-province-cma-media-media-echo-daily-flash>.
- 59 European Commission Directorate-General for European Civil Protection and Humanitarian Aid Operations (ECHO). *China Flood Updates in Henan (DG ECHO Partners)*; ECHO Daily Flash, 27 July 2021. <https://m.reliefweb.int/report/3759572/china/china-flood-updates-henan-dg-echo-partners-echo-daily-flash-27-july-2021>.
- 60 United Nations Office for the Coordination of Humanitarian Affairs (OCHA). *Yemen: Flash Update #3 – Humanitarian Impact of Flooding*; 12 August 2021. <https://reliefweb.int/report/yemen/yemen-flash-update-3-humanitarian-impact-flooding-12-august-2021-enar>.
- 61 United Nations Office for the Coordination of Humanitarian Affairs (OCHA). *Yemen: Floods*; July 2021. <https://reliefweb.int/disaster/fi-2021-000110-yem>.

- 62 United Nations Office for the Coordination of Humanitarian Affairs (OCHA). *Yemen: Flash Update #3 – Humanitarian Impact of Flooding*; 12 August 2021. <https://reliefweb.int/report/yemen/yemen-flash-update-3-humanitarian-impact-flooding-12-august-2021-enar>.
- 63 Suzuki, Y.; Kawamura, R.; Kawano, T. et al. Cascading Effects of the Changbai Mountains on an Extreme Weather Disaster in Northern Japan in January 2021. *Weather and Climate Extremes* **2022**, *36*. <https://doi.org/10.1016/j.wace.2022.100439>. See also a preliminary report by the Cabinet Office, Government of Japan on 22 February 2021 (in Japanese), [https://www.bousai.go.jp/updates/r3oyuki01/pdf/r3\\_oyuki01\\_07.pdf](https://www.bousai.go.jp/updates/r3oyuki01/pdf/r3_oyuki01_07.pdf).
- 64 United Nations Framework Convention on Climate Change (UNFCCC). *Key Aspects of the Paris Agreement* web page. [https://unfccc.int/process-and-meetings/the-paris-agreement/the-paris-agreement/key-aspects-of-the-paris-agreement#:~:text=Adaptation%20\(Art.,temperature%20goal%20of%20the%20Agreement](https://unfccc.int/process-and-meetings/the-paris-agreement/the-paris-agreement/key-aspects-of-the-paris-agreement#:~:text=Adaptation%20(Art.,temperature%20goal%20of%20the%20Agreement).
- 65 Intergovernmental Panel on Climate Change (IPCC). *Climate Change 2022: Impacts, Adaptation and Vulnerability. Contribution of Working Group II to the IPCC Sixth Assessment Report*; Pörtner, H.-O.; Roberts, D. C.; Tignor, M. et al. Eds. Cambridge University Press: Cambridge, UK and New York, USA, 2022. <https://www.ipcc.ch/report/ar6/wg2/>.
- 66 World Meteorological Organization (WMO). *2019 State of Climate Services: Agriculture and Food Security* (WMO-No. 1242). Geneva, 2019.
- 67 Economic and Social Commission for Asia and the Pacific (ESCAP). *Asia-Pacific Riskscape @ 1.5 °C: Subregional Pathways for Adaptation and Resilience – Asia-Pacific Disaster Report 2022 for ESCAP Regions: Summary for Policymakers*; United Nations: Bangkok, 2022. <https://www.unescap.org/sites/default/d8files/knowledge-products/Asia%20Pacific%20Disaster%20Report%202022%20for%20ESCAP%20Subregions%20Summary%20for%20Policymakers.pdf>; Economic and Social Commission for Asia and the Pacific (ESCAP). *Asia-Pacific Disaster Report 2021*; United Nations: Bangkok, 2021. <https://www.unescap.org/sites/default/d8files/knowledge-products/Asia-Pacific%20Disaster%20Report%202021-Full%20report.pdf>.
- 68 Biological hazards refer to climate-related biological hazards. For ESCAP analysis, these include cyclone-related diseases such as parasitic and vector diseases; drought-related diseases such as nutrition and vitamin deficiencies; flood-related diseases such as diarrheal disease; measles; and heatwave-related diseases such as cardiovascular and respiratory diseases. Disability-adjusted life year (DALY) is used as a proxy for understanding the impacts that these climate-related biological hazards could have on the population. Every one value of the DALY index represents the loss equivalent to one year of full health. Data source for DALY scores: World Health Organization (WHO). *Disability-Adjusted Life Years (DALYs) Estimates 2000–2019* web page, <https://www.who.int/data/gho/data/themes/mortality-and-global-health-estimates/global-health-estimates-leading-causes-of-dalys>.
- 69 Intergovernmental Panel on Climate Change (IPCC). Technical Summary. In *IPCC Special Report on the Ocean and Cryosphere in a Changing Climate*; Pörtner, H.-O.; Roberts, D. C.; Masson-Delmotte, V. et al. Eds.; Cambridge University Press: Cambridge, UK, and New York, USA, 2019. <https://www.ipcc.ch/srocc/>.
- 70 Economic and Social Commission for Asia and the Pacific (ESCAP). *Asia and the Pacific SDG Progress Report 2022*; United Nations: Bangkok, 2022. [https://www.unescap.org/sites/default/d8files/knowledge-products/ESCAP-2022-FG\\_SDG-Progress-Report.pdf](https://www.unescap.org/sites/default/d8files/knowledge-products/ESCAP-2022-FG_SDG-Progress-Report.pdf).
- 71 World Meteorological Organization (WMO). *WMO Atlas of Mortality and Economic Losses from Weather, Climate and Water Extremes (1970–2019)* (WMO-No. 1267). Geneva, 2021.
- 72 Global Commission on Adaptation. *Adapt Now: A Global Call for Leadership on Climate Resilience*; Global Center on Adaptation: Netherlands, and World Resources Institute: USA, 2019. [https://gca.org/wp-content/uploads/2019/09/GlobalCommission\\_Report\\_FINAL.pdf](https://gca.org/wp-content/uploads/2019/09/GlobalCommission_Report_FINAL.pdf).
- 73 United Nations Office for Disaster Risk Reduction (UNDRR). *Understanding Disaster Risk: Anticipatory Action* web page, <https://www.preventionweb.net/understanding-disaster-risk/key-concepts/anticipatory-action#pubs>.
- 74 World Meteorological Organization (WMO). *State of Climate Services: Water* (WMO-No. 1278). Geneva, 2021.
- 75 <https://www.undrr.org/implementing-sendai-framework/what-sendai-framework>
- 76 <https://rrp.unescap.org/>
- 77 <https://gcos.wmo.int/en/essential-climate-variables/>



Shared Prosperity Dignified Life



地球物理暨氣象局  
Direcção dos Serviços  
Meteorológicos e Geofísicos



المركز الوطني للأرصاد  
National Center for Meteorology  
المملكة العربية السعودية



NCM  
المركز الوطني للأرصاد  
National Center of Meteorology



For more information, please contact:

## World Meteorological Organization

7 bis, avenue de la Paix – P.O. Box 2300 – CH 1211 Geneva 2 – Switzerland

Strategic Communications Office

Tel.: +41 (0) 22 730 83 14 – Fax: +41 (0) 22 730 80 27

Email: [cpa@wmo.int](mailto:cpa@wmo.int)

[public.wmo.int](http://public.wmo.int)